bioRxiv preprint doi: https://doi.org/10.1101/129353; this version posted April 29, 2017. The copyright holder for this preprint (which was not certified by peer review) is the author/funder, who has granted bioRxiv a license to display the preprint in perpetuity. It is made available under aCC-BY 4.0 International license.

Ranking quantitative resistance to Septoria tritici blotch in elite wheat cultivars using automated image analysis

Petteri Karisto, Andreas Hund, Kang Yu, Jonas Anderegg, Achim Walter, Fabio Mascher, Bruce A. McDonald, and Alexey Mikaberidze

First, seventh and eighth authors: Plant Pathology Group, Institute of Integrative Biology, ETH Zurich, Zurich, Switzerland; second, third, fourth and fifth authors: Crop Science Group, Institute of Integrative Biology, ETH Zurich, Zurich, Switzerland; sixth author: Plant Breeding and Genetic Resources, Institute for Plant Production Sciences, Agroscope, Nyon, Switzerland

Corresponding author: P. Karisto;
E-mail address: petteri.karisto@usys.ethz.ch

bioRxiv preprint doi: https://doi.org/10.1101/129353; this version posted April 29, 2017. The copyright holder for this preprint (which was not certified by peer review) is the author/funder, who has granted bioRxiv a license to display the preprint in perpetuity. It is made available under aCC-BY 4.0 International license.

Abstract

Quantitative resistance is likely to be more durable than major gene resistance for controlling Septoria tritici blotch (STB) on wheat. Earlier studies hypothesized that resistance affecting the degree of host damage, as measured by the percentage of leaf area covered by STB lesions, is distinct from resistance that affects pathogen reproduction, as measured by the density of pycnidia produced within lesions. We tested this hypothesis using a collection of 335 elite European winter wheat cultivars that was naturally infected by a diverse population of *Zymoseptoria tritici* in a replicated eld experiment. We used automated analysis of 21214 scanned wheat leaves to obtain quantitative measures of STB conditional severity that were precise, objective, and reproducible. These measures allowed us to explicitly separate resistance affecting host damage from resistance affecting pathogen reproduction, enabling us to confirm that these resistance traits are largely independent. The cultivar rankings based on host damage were different from the rankings based on pathogen reproduction, indicating that the two forms of resistance should be considered separately in breeding programs aiming to increase STB resistance. We hypothesize that these different forms of resistance are under separate genetic control, enabling them to be recombined to form new cultivars that are highly resistant to STB. We found a significant correlation between rankings based on automated image analysis and rankings based on traditional visual scoring, suggesting that image analysis can complement conventional measurements of STB resistance, based largely on host damage, while enabling a much more precise measure of pathogen reproduction. We showed that measures of pathogen reproduction early in the growing season were the best predictors of host damage late in the growing season, illustrating the importance of breeding for resistance that reduces pathogen reproduction in order to minimize yield losses caused by STB. These data can already be used by breeding programs aiming to increase STB resistance to choose wheat cultivars that are broadly resistant to naturally diverse *Z. tritici* populations according to the different classes of resistance.

bioRxiv preprint doi: https://doi.org/10.1101/129353; this version posted April 29, 2017. The copyright holder for this preprint (which was not certified by peer review) is the author/funder, who has granted bioRxiv a license to display the preprint in perpetuity. It is made available under aCC-BY 4.0 International license.

Zymoseptoria tritici (Desm.) Quaedvlieg & Crous (formerly *Mycosphaerella graminicola* (Fuckel) J. Schröt. in Cohn) is a fungal pathogen that poses a major threat to wheat production globally (Jorgensen et al., 2014; Dean et al., 2012). It infects wheat leaves, causing the disease Septoria tritici blotch (STB). The yield loss posed by STB can be 5-10%, even when resistant cultivars and fungicides are used in combination, and around 1.2 billion dollars are spent annually on fungicides targeted mainly towards STB control in Europe alone (Torriani et al., 2015). *Z. tritici* has a highly diverse and dynamic population that carries a high degree of fungicide resistance in Europe (reviewed in Fones and Gurr, 2015; Torriani et al., 2015). In several cases, fungicides repeatedly lost their efficacy only a few years after their introduction due to rapid emergence of fungicide-resistant strains of *Z. tritici* (Griffin and Fisher, 1985; Fraaije et al., 2005; Torriani et al., 2009). Resistance to azoles, an important class of fungicides that is widely used to control STB, has been growing steadily over the last twenty years (Cools and Fraaije, 2013; Zhan et al., 2006) and appeared recently in North America (Estep et al., 2015). Therefore, STB-resistant wheat cultivars have become an important breeding objective to enable more effective management of the disease (McDonald and Mundt, 2016). Major resistance genes such as STB6 (Brading et al., 2002) provide nearly complete resistance against a subset of *Z. tritici* strains carrying the wild type AvrStb6 allele (Zhong et al., 2017), but as found for fungicides, major resistance often breaks down a few years after it is introduced. Quantitative resistance may be conferred by a large number of quantitative trait loci (QTLs) with small and additive effects that can be combined to provide high levels of disease resistance (Poland et al., 2009; St. Clair, 2010; Kou and Wang, 2010; McDonald and Linde, 2002; Mundt, 2014). Quantitative resistance is thought to be more durable and hence deserves more attention from breeders (McDonald and Linde, 2002; St. Clair, 2010; Mundt, 2014).

To enable breeding for quantitative resistance to STB, we need to comprehensively analyze the quantitative distribution of its associated phenotypes, which is much more difficult than phenotyping major gene resistance that typically shows a binomial distribution. This challenge was recognized more than forty years ago and a number of studies were conducted to evaluate quantitative resistance to STB under field conditions using artificial inoculation (Rosielle, 1972; Shaner and Finney, 1982; Eyal, 1992; Brown et al., 2001; Miedaner et al., 2013) and natural infection (Rosielle, 1972; Shaner et al., 1975; Miedaner et al., 2013; Kollers et al., 2013*b*). Resistance to STB was also investigated on detached leaves with artificial inoculations [e. g., by Chartrain et al. (2004)]. Several studies performed visual scoring of quantitative resistance only once during the growing season (Rosielle, 1972; Shaner and Finney, 1982; Eyal, 1992; Miedaner et al., 2013), while other studies included two or more time points (Shaner et al., 1975; Brown et al., 2001; Kollers et al., 2013*b*). One of the most comprehensive early studies screened 7500 wheat varieties including 2000 durum wheat cultivars to select the 460 most resistant varieties for more detailed visual scoring (Rosielle, 1972).

Understanding the infection cycle of STB helps to distinguish and measure most important aspects of quantitative resistance to the disease. *Z. tritici* spores germinate on wheat leaves and penetrate the leaves through stomata (Kema et al., 1996). After penetration, fungus grows for several days latently within leaves producing no visible

bioRxiv preprint doi: https://doi.org/10.1101/129353; this version posted April 29, 2017. The copyright holder for this preprint (which was not certified by peer review) is the author/funder, who has granted bioRxiv a license to display the preprint in perpetuity. It is made available under aCC-BY 4.0 International license.

symptoms. During the latent phase, *Z. tritici* grows in apoplast and invades host mesophyll around the position of initial penetration (Duncan and Howard, 2000). After some ten days growth of fungus becomes necrotrophic, necrotic lesions appear in the invaded host tissue and asexual fruiting bodies, pycnidia, begin to form (Kema et al., 1996; Duncan and Howard, 2000). In dead host tissue the fungus grows saprotrophically and produces sexual fruiting bodies, pseudotechia, 25-30 days after infection (Sánchez-Vallet et al., 2015). Whether *Z. tritici* is best referred to as a hemibiotroph or a latent necrotroph is ambiguous (Sánchez-Vallet et al., 2015). Asexual pycnidiospores are usually spread by rain splash and sexual ascospores are spread by wind. The pathogen typically undergoes up to 5-6 rounds of asexual and 1-2 rounds of sexual reproduction per growing season.

Incidence of STB depends on the number of spores that attempt to infect healthy leaves and the infection efficiency. Overall severity of infection depends on both of these factors and additionally on the ability of the pathogen to damage the host tissue once infected. Studies of Zhan et al. (1998) and Zhan et al. (2000) indicate that ≈66% of infections on flag leaves came from asexual spores, while ≈24% came from ascospores originating from within the infected field and 10% of infections were immigrants from surrounding fields. Pathogen asexual reproduction is thus the most important factor explaining infection on flag leaves. The amount of necrosis induced by STB on uppermost leaves determines yield losses (Brokenshire, 1976).

Earlier studies of STB resitance (reviewed above) combined disease severity and incidence using visual assessments based on categorical scales. In studies of Rosielle (1972), Shaner et al. (1975) and Eyal (1992) these scales included both the degree of lesion coverage and the density of pycnidia in lesions, but in studies of Brown et al. (2001) and Chartrain et al. (2004) the disease scores were based on leaf coverage by lesions bearing pycnidia (i. e. using a presence/absence measurement of pycnidia). The accuracy of this method is limited by an inherent subjective bias and a small number of qualitative categories, which may impair success of breeding.

In several studies the importance of the resistance component that suppresses pathogen reproduction (production of pycnidia) was recognized based on qualitative observations of pycnidial coverage [e. g., (Rosielle, 1972; Shaner et al., 1975; Shaner and Finney, 1982)]. Manual counting of pycnidia is extremely labor-intensive, though, so it was only feasible to count pycnidia on a small scale [e. g., (Shaner et al., 1975)] because there was no technology available to automate this process.

Automated image analysis (AIA) has been used in the past for example for analysis of liver tissue (e. g. O'Gorman et al., 1985) and breast tissue (e. g. Phukpattaranont and Boonyaphiphat, 2007) and for analysis of land use (e. g. Drăguţ and Blaschke, 2006). AIA provides a promising tool for measuring quantitative disease resistance in the field (Mahlein, 2016; Simko et al., 2017). Mutka and Bart (2015) and Mahlein (2016) highlight importance of standardized imaging methods for reproducibility. We used a novel phenotyping method based on automated analysis of scanned leaf images (Stewart and McDonald, 2014; Stewart et al., 2016) in a wheat panel planted to 335 European cultivars in a replicated field experiment (Kirchgessner et al., 2017). The method benefits from well defined procedure of detaching leaves and scanning them in standardized conditions,

bioRxiv preprint doi: https://doi.org/10.1101/129353; this version posted April 29, 2017. The copyright holder for this preprint (which was not certified by peer review) is the author/funder, who has granted bioRxiv a license to display the preprint in perpetuity. It is made available under aCC-BY 4.0 International license.

thus leading to objective and reproducible results. Additionally, it enables generation of large amounts of reliable data at a relatively low cost.

Importantly, our method allowed us to separate quantitative resistance traits affecting host damage caused by the pathogen from resistance traits related to pathogen reproduction on a large scale and with a high accuracy. Pathogen reproduction was quantified by automatic counting of asexual fruiting bodies of the pathogen (pycnidia) on wheat leaves (Stewart and McDonald, 2014; Stewart et al., 2016).

In this large-scale field experiment, leaves were infected naturally by a genetically diverse local *Z. tritici* population and the epidemic was allowed to develop naturally. Despite three fungicide treatments including five active ingredients that eliminated virtually all other diseases, the level of STB infection was widespread across the field experiment. This pervasive natural infection by a fungicide-resistant population allowed us to investigate quantitative resistance in a nearly pure culture of *Z. tritici* under field conditions. The combination of wet and cool weather conditions favoring development of STB, a large number of wheat cultivars planted in a single location, and utilization of a novel automated digital image analysis method enabled a multi-dimensional and comprehensive characterization of quantitative resistance that led to a clear ranking of STB resistance in a broad collection of European winter wheat cultivars.

We report separate rankings of wheat cultivars based on two different resistance components, one acting against host damage and the other acting against pathogen reproduction. We found that the two rankings are considerably different. We identified a phenotypic quantity that combines these two components and found that it correlates with the ranking based on traditional visual assesments. In this way, we identified new, broadly active sources of resistance to STB in existing European wheat cultivars. Our outcomes open several possibilities for further genetic studies of quantitative resistance to STB.

Materials and Methods

Plant materials and experimental design. A total of 335 elite European winter wheat (*Triticum aestivum*) varieties from the GABI-wheat panel (Kollers et al., 2013*a*,*b*) were evaluated in this experiment. Two replicates of the wheat panel were grown during the 2015–2016 growing season in two complete blocks separated by 100 meters at the Field Phenotyping Platform site of the Eschikon Field Station of the ETH Zurich, Switzerland (coordinates 47.449683, 8.682461) (Kirchgessner et al., 2017). The complete blocks represented two different lots in the FIP. Within each lot the genotypes were arranged in incomplete blocks in row and range direction and a check variety (CH Claro) was repeated at least once within each row and range. Cultivars were planted in a single 1.2m×1.7m plot within each lot except for cultivar CH Claro having 21 replicates within each lot. All cultivars were sown on 13 October 2015.

Standard agricultural practices were used including applications of fertilizers and pesticides. Fertilizers were applied five times during spring 2016, including boron with ammonium nitrate (nitrogen 52 kg/ha) on 4 March; P_2O_5 at 92 kg/ha on 7 March; K_2O

bioRxiv preprint doi: https://doi.org/10.1101/129353; this version posted April 29, 2017. The copyright holder for this preprint (which was not certified by peer review) is the author/funder, who has granted bioRxiv a license to display the preprint in perpetuity. It is made available under aCC-BY 4.0 International license.

at 120 kg/ha on 10 March; magnesium with ammonium nitrate on 12 April (magnesium 15 kg/ha, nitrogen 72 kg/ha) and 20 May (magnesium 4 kg/ha, nitrogen 19 kg/ha). The pre-emergence herbicide Herold SC (Bayer) was applied on 29 October 2015 (dose 0.6 l/ha); stem shortener Moddus (Syngenta) was applied on 6 April 2016 [dose 0.4 l/ha, GS (growth stage) 31 (Zadoks et al., 1974)]. Insecticide Biscaya (Bayer) was applied on 25 May, 2016 (dose 0.3 l/ha, GS 51). Fungicides were applied three times: (i) 6 April, 2016, Input, Bayer (a mixture of the active ingredients spiroxamin at 300 g/l and prothioconazole at 150 g/l, dose 1.25 l/ha, GS 31); (ii) 25 May, Aviator Xpro, Bayer (a mixture of bixafen at 75 g/l and prothiconazole at 150 g/l, dose 1.25 l/ha, GS 51) and 6 June, Osiris, BASF (a mixture of epoxiconazole at 56.25 g/l and metconazole at 41.25g/l, dose 2.5 l/ha, GS 65). In total, the three fungicide applications included five active ingredients representing three modes of action.

STB inoculum and calculation of number of cycles of infection. All STB infection was natural, with the majority of primary inoculum likely originating from airborne ascospores coming from nearby wheat fields that surround the Eschikon field site. We estimated the number of asexual cycles of pathogen reproduction by using the data from Shaw (1990) showing the effect of temperature on latent period and local weather data coming from the nearby Lindau weather station (see Appendix A.1 for details of estimation).

Disease assessment based on automated image analysis. Leaves exhibiting obvious STB lesions were collected two times during the growing season. The first collection was made on 20 May 2016 (t_1, approximately GS 41) and the second collection was made on 4 July 2016 (t_2, approximate GS are in the range 75-85). For both collections, 16 infected leaves were collected at random from each plot. At t_1, leaves were collected from the highest infected leaf layer, which was typically the third or fourth fully extended, but non-senescent leaf still visible when counting from the ground. At t_2, the leaf layer below the flag leaf (F-1) was sampled in each plot. The sampled leaves were placed in paper envelopes, kept on ice in the field, and stored at 4° C for two days before mounting on A4 paper with printed reference marks and sample names, as described in (Stewart et al., 2016). Absorbent paper was placed between each sheet of eight mounted leaves and sheets were pressed with approximately 5 kg at 4° C for two-three days prior to scanning at 1200 dpi with a Canon CanoScan LiDE 220 flatbed scanner. The resulting scans were saved as "jpeg" images.

Scanned images were analyzed with the software ImageJ (Schindelin et al., 2015) using a specialized macro described in Stewart and McDonald (2014) and Stewart et al. (2016)(source code of the macro and a user manual are given in (Stewart et al., 2016)). The parameters used for the macro are given in supplemental Table S1 and an explanation of their meaning is provided in the macro instructions in (Stewart et al., 2016). Figure 1 illustrates the workflow associated with the macro. The maximum length of the scanned area for each leaf was 17 cm. When leaves were longer than 17 cm, bases of the leaves were placed within the scanned area, while the leaf tips extended outside

bioRxiv preprint doi: https://doi.org/10.1101/129353; this version posted April 29, 2017. The copyright holder for this preprint (which was not certified by peer review) is the author/funder, who has granted bioRxiv a license to display the preprint in perpetuity. It is made available under aCC-BY 4.0 International license.

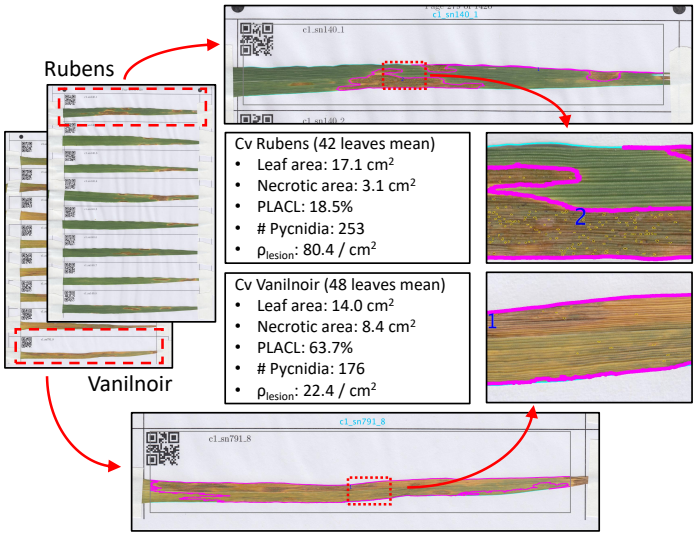

Figure 1: Illustration of the phenotyping procedure with the ImageJ macro (Stewart et al., 2016). Leaves are mounted on paper sheets; the ImageJ macro distinguishes leaves from white background; within each leaf, the macro identifies necrotic lesions and their areas; within each lesion, the macro identifies pycnidia (black dots) and measures their areas and gray values (degree of melanization).

Table 1: Important STB disease properties determined using automated image analysis.

Quantity	Description	Dimension
PLACL	percentage of leaf area covered by lesions	percent
ρ_{lesion}	density of pycnidia per unit lesion area	# pycnidia/cm^2 lesion
ρ_{leaf}	density of pycnidia per unit total leaf area	# pycnidia/cm^2 leaf

the scanned area. For each leaf, the following quantities were automatically recorded from the scanned image: total leaf area, necrotic leaf area, number of pycnidia and their positions, size and gray value of each pycnidium. From these measurements, the percentage of leaf area covered by lesions (PLACL), the density of pycnidia per unit lesion area (ρ_{lesion}), the density of pycnidia per unit leaf area (ρ_{leaf}), the mean pycnidia gray value and the mean pycnidia sizes were calculated.

The three quantities PLACL, ρ_{lesion}, and ρ_{leaf} quantify different aspects of STB conditional severity in each plot, but did not provide overall measurements of STB incidence because only 16 leaves were measured. Although we aimed to collect only infected leaves, there were a few cases in plots with very little STB when the collected leaves did not have necrotic lesions or did not have pycnidia. These leaves were not considered when calculating the mean or median values used for ranking cultivars or assessing the magnitude of effects.

To confirm the outcomes of the automated image analysis, we visually examined about 1440 leaves (about 5 % of all sampled leaves) to compare scanned leaf images with overlay

bioRxiv preprint doi: https://doi.org/10.1101/129353; this version posted April 29, 2017. The copyright holder for this preprint (which was not certified by peer review) is the author/funder, who has granted bioRxiv a license to display the preprint in perpetuity. It is made available under aCC-BY 4.0 International license.

images in which detected lesions and pycnidia are marked by the macro (examples of overlays are shown in Fig. 1). We included in this analysis about 1100 leaves from the 20 cultivars that exhibited the largest difference in their overall rankings with respect to PLACL and ρ_{lesion} as well as about 140 leaves with outlier values for ρ_{lesion} and mean pycnidial area.

For each leaf subjected to visual inspection, we determined whether the macro correctly detected lesions and pycnidia. In cases with errors, we determined the cause of the error. Errors that led to incorrect quantification of disease symptoms could be divided into four categories: defects on leaves, collector bias, scanning errors and deficiencies in the image analysis software (the macro). Leaf defects included insect damage, mechanical damage, insect bodies and frass, other fungi, uneven leaf surfaces creating shadows, and dust particles on leaves. We identified several cases of biased leaf collection at t_1, where leaves were sampled from lower leaf layers in which most of the leaf surface exhibited natural senescence, leading to extensive chlorosis and some necrosis. (Data from 20 plots in collection t_1 was removed due to strong collector bias during the initial quality control after collection). Scanning errors included shadows on leaf edges and folded leaves. Deficiencies of the macro consisted of recognizing green parts of leaves as lesions, dark spaces between light-colored leaf hairs and parts of dark borders around lesions as pycnidia. In total, 336 leaves were deemed to exhibit scoring errors and removed from the dataset as a result of this procedure.

We estimated the total proportion of scoring errors as $p_{\text{tot}} = 0.15 \pm 0.05$ by careful visual examination $n = 200$ leaves which were chosen randomly with replacement from the entire sample of 21551 leaves. The proportion of scoring errors due to collector bias was estimated as $p_{\text{cb}} = 0.055 \pm 0.003$. Here, the uncertainties are reported in the form of the 95 % confidence intervals calculated according to $CI = 1.96\sqrt{p(1-p)/n}$, where p is the sample proportion and n is the sample size.

Disease assessment based on visual scoring. Visual assessments of STB were performed at three time points: 20 May (approximately GS 41), 21 June (approximately GS 75) and 29 June (approximately GS 80). STB level in each plot was scored on the three uppermost leaf layers on a 1-9 scale (1 means no disease, 9 means complete infection) based on both STB incidence and severity. The presence of pycnidia was used as an indicator of STB infection. The absence of pycnidia was interpreted as an absence of STB, even if necrotic lesions were visible. During visual scoring, the presence of other diseases (such as stripe rust, septoria nodorum bloth and fusarium head blight) was assessed qualitatively. All plots were scored with approximately equal time spent on each plot.

Statistical analysis. We compared differences in STB resistance among cultivars for each dataset by pooling together the data points from individual leaves belonging to different replicates and sampling dates. The data from the automated image analysis consisted of ≈60 data points per cultivar representing the two time points and two biological replicates. The visual scoring data was based on three time points and two

bioRxiv preprint doi: https://doi.org/10.1101/129353; this version posted April 29, 2017. The copyright holder for this preprint (which was not certified by peer review) is the author/funder, who has granted bioRxiv a license to display the preprint in perpetuity. It is made available under aCC-BY 4.0 International license.

biological replicates generating ≈6 data points per cultivar. Cultivar CH Claro was an exception because it was replicated 42 times and thus had ≈1300 data points from leaf image analysis and 120 data points from visual scoring. The relative STB resistance of all wheat cultivars was ranked based on means of PLACL, ρ_{lesion} and ρ_{leaf} over ≈60 individual leaf data points. We also calculated medians and standard errors of means for each cultivar.

For each cultivar the area under disease progress curve (AUDPC) was calculated by taking averages of visual scores over the two replicates. It was assumed that infection started from zero at 14 days before the first assessment. To analyze differences between cultivars these scores were weighted with coefficients that depend on times of assessments such that each weighted score gives a proportional contribution to the total AUDPC and the average over scores from different replicates and time points gives the total AUDPC (see Appendix A.2 for details on calculation of AUDPC and weighting of scores). AUDPC was used to rank cultivars according to visual scoring (Fig. 3D).

The significance of differences in resistance between cultivars was tested with the global Kruskal-Wallis test (Sokal and Rohlf, 2012) using kruskal.test function in R (R Core Team, 2016) on each data set. For resistance measures showing global differences between cultivars, we determined significantly different groups of cultivars based on pairwise comparisons, so that any two cultivars in the same group are not significantly different from each other and any two cultivars from different groups are different. Pairwise differences were tested with multiple pairwise Kruskal-Wallis tests using the function kruskal in the package agricolae in R (de Mendiburu, 2016) using the false discovery rate (FDR) 0.05 for significance level correction (Benjamini and Hochberg, 1995) for multiple comparisons.

We determined correlations between cultivar rankings based on AUDPC and both means and medians of PLACL, ρ_{lesion} and ρ_{leaf} for each cultivar. We also computed correlations with respect to means of PLACL, ρ_{lesion} and ρ_{leaf} between t_1 and t_2 to determine the predictive power of these quantities. In this case, means were taken over about 16 leaves originating from the same plot. All correlations were calculated with the help of Spearman's correlation test (Sokal and Rohlf, 2012) using the open-source scipy package (http://www.scipy.org) written for the Python programming language (http://www.python.org).

We analyzed differences between t_1 and t_2 in terms of PLACL, ρ_{lesion} and ρ_{leaf} to identify cultivars whose resistance increased over time. For this purpose, we used the Wilcoxon rank sum test with the FDR correction for multiple comparisons ($p < 0.01$).

Results

Overall description of the STB epidemic. Despite three fungicide applications with five active ingredients and three modes of action, we observed widespread STB in nearly all of the experimental plots. There were obvious differences in overall levels of STB infection on different cultivars. Comparison of overall levels of STB disease with nearby untreated plots showed that the fungicides significantly suppressed STB development.

bioRxiv preprint doi: https://doi.org/10.1101/129353; this version posted April 29, 2017. The copyright holder for this preprint (which was not certified by peer review) is the author/funder, who has granted bioRxiv a license to display the preprint in perpetuity. It is made available under aCC-BY 4.0 International license.

STB was the dominating disease in the fungicide-treated plots; other leaf diseases were present at very low levels as a result of the fungicide treatments. Hence this experiment provided an unusual opportunity to assess quantitative STB resistance to a natural infection and under field conditions in the absence of competing wheat diseases.

According to weather data collected from the Lindau weather station located about 200 m away from the field site, the weather in spring-summer 2016 was cool and rainy, highly conducive to development of STB (see Fig. A2 in Appendix A.1). Average daily temperature between 1 March and 27 July was 12.5^o C and the total amount of rainfall was 1245 mm. Based on daily temperature and rainfall data, we estimated the number of *Z. tritici* asexual generations over the growing season as six. Between the two sampling dates t_1 and t_2, we estimated two asexual generations (see Appendix A.1 for details of estimation).

An overview of the dataset. A total of 21214 leaves were included in the automated analysis pipeline, with an average of 30 leaves per plot. The total leaf area analyzed was 36.9 m^2 of which 11.2 m^2 was recognized as damaged by STB. The mean analyzed area of an individual leaf was 17 cm^2. In total 5.1 million pycnidia were counted and analyzed for size and gray value. The mean number of pycnidia within a leaf was 243. A more detailed description of the overall dataset is given in Table 2. The full dataset can be accessed from xxx. Correlations between the two biological replicates ranged from 0.3 to 0.7 (Fig. A3, see Appendix A.3 for more details).

The distributions of the raw data points corresponding to individual leaves with respect to PLACL, ρ_{lesion} and ρ_{leaf} are shown in Figs. 2 and 3 (the full range of ρ_{lesion} and ρ_{leaf} is shown in Figs. E2.1 and E2.2). The distributions of PLACL, ρ_{lesion} and ρ_{leaf} were non-normal and had outliers. All of these distributions were continuous, consistent with previous studies that hypothesized that the majority of STB resistance in wheat is quantitative (Stewart et al., 2016).

For the visual assessments conducted across two replicates and three time points, the lowest score was 1 and the highest score was 4 (on a 1-9 scale). The lowest value of the AUDPC was 81, the highest value was 154 and the average AUDPC across all cultivars was 103.

The visual assessment found that yellow rust was present in about 1 % of plots on 20 May and in about 2 % of plots on 21 June, 2016; Septoria nodorum blotch was present in only a single plot on 21 June, 2016 (about 0.1 % of plots); Fusarium head blight was present in about 2 % of plots only on 21 June, 2016.

Host damage vs. pathogen reproduction. From the raw data obtained via automated analysis of scanned leaves, we derived three quantitative resistance measures: PLACL, ρ_{lesion} and ρ_{leaf}. PLACL is defined as the necrotic leaf area divided by the total leaf area, ρ_{lesion} is the total number of pycnidia divided by the necrotic leaf area and ρ_{leaf} is the total number of pycnidia divided by the total leaf area. ρ_{leaf} can also be calculated from

bioRxiv preprint doi: https://doi.org/10.1101/129353; this version posted April 29, 2017. The copyright holder for this preprint (which was not certified by peer review) is the author/funder, who has granted bioRxiv a license to display the preprint in perpetuity. It is made available under aCC-BY 4.0 International license.

Table 2: Summary of the leaf analysis

	Total	Mean	Median	Maximum	Minimum
Measured quantities					
Leaf area (mm^2)	36 874 893	1738	1701	3626	103
Necrotic area (mm^2)	11 162 727	526	415	2519	0
Number of pycnidia	5 148 640	243	147	4828	0
Pycnidia area (mm^2)	77 681	3.66	2.35	56	0
Derived quantities					
PLACL (%)		32	24	99.6	0
ρ_{lesion}		48	40	416	0
ρ_{leaf}		14	9	301	0

the first two factors as

$$\text{PLACL} \cdot \rho_{\text{lesion}} = \frac{\text{Necrotic area}}{\text{Leaf area}} \cdot \frac{\text{Number of pycnidia}}{\text{Necrotic area}} = \frac{\text{Number of pycnidia}}{\text{Leaf area}} = \rho_{\text{leaf}}. \tag{1}$$

PLACL characterizes host damage due to pathogen while ρ_{lesion} characterizes pathogen reproduction on the necrotic leaf tissue. ρ_{leaf} is the product of these two quantities, combining both host damage and pathogen reproduction. Independent identification of these three quantities from the raw leaf data allowed us to differentiate between host damage and pathogen reproduction, and also to combine these two factors into the most integrative measure of disease severity. In this way, we gained a comprehensive insight into different components of disease severity. Next, we rank wheat cultivars with respect to each of these three quantities.

Ranking of cultivars. Resistance ranking of the cultivars was based on the three measures obtained from automated image analysis (PLACL, ρ_{lesion} and ρ_{leaf}) and the AUDPC calculated from visual scoring. For PLACL, ρ_{lesion} and ρ_{leaf}, the distributions differed significantly between cultivars. For each of these three measures, the null hypothesis of identical distributions for all cultivars was rejected by a Kruskal-Wallis global comparison with $p < 2.2 \cdot 10^{-16}$. However, the global Kruskal-Wallis test did not reveal differences between distributions of the weighted visual scores ($p = 1$). Kruskal-Wallis multiple pairwise comparisons identified three significantly different groups of cultivars for both PLACL and ρ_{lesion} and four significantly different groups of cultivars for ρ_{leaf} (Figs. 2 and 3). Supplemental File S3 shows that mean ranks are highly correlated with the means and medians, indicating that in the majority of cases significantly different cultivars also have different means and medians.

There were notable changes between resistance rankings based on PLACL and ρ_{lesion} (black lines in Fig. 2D). Several of the thirty least resistant cultivars based on host damage were ranked among the most resistant cultivars based on pathogen reproduction. Similarly, some of the most resistant cultivars based on host damage were among the least resistant cultivars based on pathogen reproduction. For example cultivar Vanil-

bioRxiv preprint doi: https://doi.org/10.1101/129353; this version posted April 29, 2017. The copyright holder for this preprint (which was not certified by peer review) is the author/funder, who has granted bioRxiv a license to display the preprint in perpetuity. It is made available under aCC-BY 4.0 International license.

noir showed high PLACL and low ρ_{lesion} whereas cultivar Rubens exhibited the opposite pattern. Visual examination of leaves belonging to cultivars that exhibited the largest difference in their ranking between PLACL and ρ_{lesion} confirmed qualitatively the presence of the effect. We observed high degree of necrosis and low numbers of pycnidia in cultivars that ranked high in terms of PLACL and low in terms of ρ_{lesion}. We also confirmed that cultivars that ranked high in terms of ρ_{lesion} and low in terms of PLACL had on average a low degree of necrosis and high numbers of pycnidia. These qualitative observations represent a general quantitative pattern, as indicated by relatively low correlations between PLACL and ρ_{lesion} with respect to means ($r_{\text{s}} = 0.1$, $p = 0.059$, Fig. 2G) and medians ($r_{\text{s}} = 0.18$, $p = 0.0007$, Fig. 2F) taken over leaves belonging to the same cultivar. On the contrary, the correlation between PLACL and ρ_{lesion} was negative and highly significant when calculated based on individual leaf data pooled together ($r_{\text{s}} = -0.1$, $p = 1.9 \cdot 10^{-53}$, Fig. 2H). Supplemental Tables S2–5 supporting Fig. 2 show means, standard errors of means, medians and Kruskall-Wallis test statistics based on PLACL and ρ_{lesion} for all cultivars. Supplemental File S1 gives brief description of all supplemental files and tables.

Automated measures of quantitative STB resistance correlate strongly with the traditional measurement based on AUDPC of visual scores. Medians of PLACL and ρ_{lesion} correlated significantly ($p < 10^{-10}$) with the AUDPC ($r_s = 0.37$ and $r_s = 0.49$ respectively). Correlations between AUDPC and means were somewhat weaker but also significant. The strongest correlation was between the combined measure ρ_{leaf} and the AUDPC (cf. Fig. 3, means: $r_s = 0.6$, medians: $r_s = 0.54$). More figures of cultivar ranking that support Figs. 2 and 3 with different measure combinations are shown in Supplemental File S2. Supplemental Tables 6–7 supporting Fig. 3 show means, standard errors of means, medians and Kruskall-Wallis test statistics based on ρ_{leaf} for all cultivars.

Predictors of epidemic development. So far we analyzed data for each cultivar based on pooling both sampling dates t_1 and t_2. Next we consider data from the sampling dates t_1 and t_2 separately. An important question is: To what extent can we predict a measure of disease at t_2 from measurements made at t_1? We address this question by investigating correlations between t_1 and t_2 with respect to each of the three measures: PLACL, ρ_{lesion}, and ρ_{leaf} (Fig. 4). A higher degree of correlation corresponds to a higher predictive power.

Consider the first column in Fig. 4 that illustrates how PLACL in t_1 correlates with PLACL, ρ_{lesion} and ρ_{leaf} in t_2. PLACL in t_1 correlates somewhat better with ρ_{lesion} in t_2 than with ρ_{leaf} or PLACL in t_2. But PLACL in t_1 is a poorer predictor for the three quantities in t_2 than the quantities that include pycnidia counts, ρ_{lesion} and ρ_{leaf} (compare first column with second and third columns in Fig. 4). The highest correlations emerge between ρ_{lesion} in t_1 and ρ_{leaf} in t_2 ($r_{\text{s}} = 0.36$); between ρ_{leaf} in t_1 and ρ_{leaf} in t_2 ($r_{\text{s}} = 0.37$); and between ρ_{leaf} in t_1 and ρ_{lesion} in t_2 ($r_{\text{s}} = 0.39$). As we see from the first row in Fig. 4, the best predictor for PLACL (the measure of host damage that is most likely to reflect decreased yield) in t_2 is ρ_{lesion} (the most inclusive measure of pathogen

bioRxiv preprint doi: https://doi.org/10.1101/129353; this version posted April 29, 2017. The copyright holder for this preprint (which was not certified by peer review) is the author/funder, who has granted bioRxiv a license to display the preprint in perpetuity. It is made available under aCC-BY 4.0 International license.

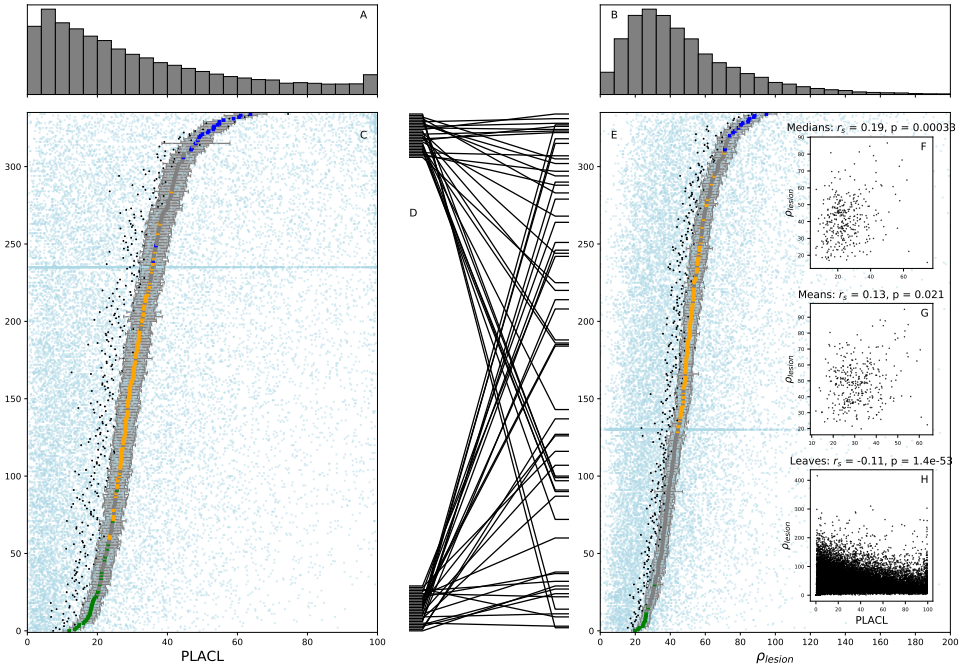

Figure 2: Ranking of wheat cultivars according to resistance against host damage (panel C) and pathogen reproduction (panel E). Wheat cultivars are ranked in order of increasing susceptibility to STB based on mean values of PLACL (percentage of leaf area covered by lesions, panel C) and ρ_{lesion} (panel E). Colored markers depict means over two replicates and two time points, error bars indicate standard errors of means. Different colors of markers (blue, red, green) represent significantly different groups of cultivars based on Kruskal-Wallis multiple comparison FDR correction, gray dots correspond to cultivars that could be assigned to any group. Light blue dots represent average values for individual leaves. Cultivar CH Claro appears as a horizontal blue line due to its 21-fold higher number of replicates. Black dots show medians for each cultivar. Lines in panel D represent changes in ranking between PLACL and ρ_{lesion} among the 30 most susceptible and the 30 most resistant cultivars. Panels A and B show frequency histograms of PLACL and ρ_{lesion} based on individual leaf data from two replicates and two time points. Three insets in panel E illustrate the relationship between PLACL and ρ_{lesion} based on individual leaf data (panel H), means (G) and medians (panel F). Panels B and E extend only up to 200 along the x-axis, missing 82 data points with values between 200 and 416.

bioRxiv preprint doi: https://doi.org/10.1101/129353; this version posted April 29, 2017. The copyright holder for this preprint (which was not certified by peer review) is the author/funder, who has granted bioRxiv a license to display the preprint in perpetuity. It is made available under aCC-BY 4.0 International license.

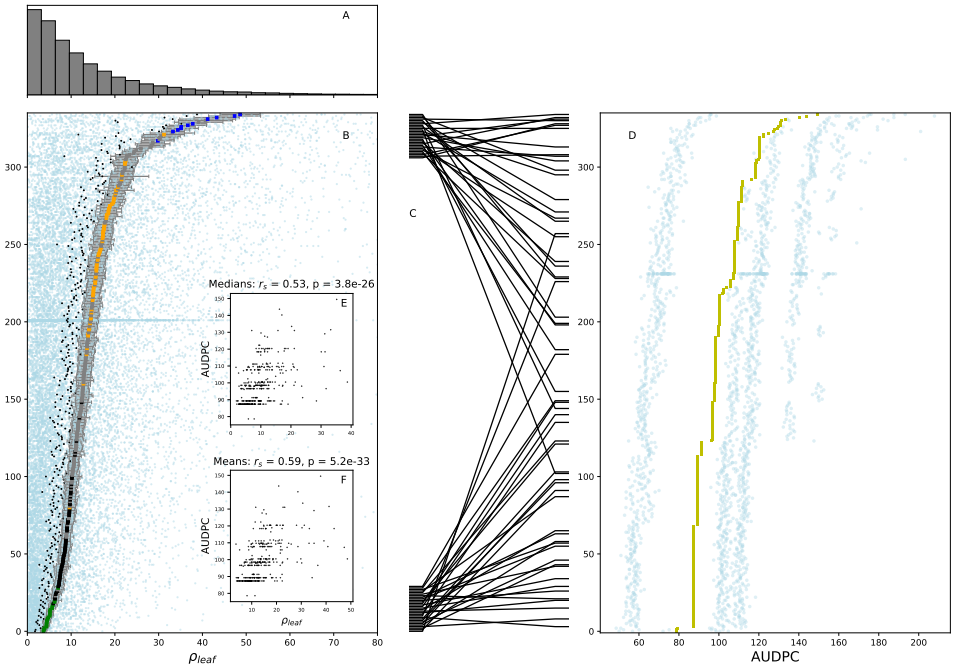

Figure 3: Ranking of wheat cultivars according to the resistance measure, ρ_{leaf}, that combines host damage and pathogen reproduction (panel B) and according to AUDPC (area under the disease progress curve) based on conventional visual assessments (panel D). In panels B and D cultivars are ranked in order of increasing susceptibility based on mean values of leaf pycnidia density, ρ_{leaf} (panel B), and AUDPC (panel D). Colored markers show means over two replicates and two time points, error bars indicate standard errors of means. Different colours of markers (blue, red, black, green) represent significantly different groups of cultivars based on a Kruskal-Wallis multiple comparison with FDR correction, gray dots correspond to cultivars that could not be assigned to any group. Light blue dots represent average values for individual leaves. Cultivar CH Claro appears as a horizontal blue line due to its 21-fold higher number of replicates. Black dots show medians for each cultivar. Lines in panel C represent changes in ranking between ρ_{leaf} and AUDPC among the 30 most susceptible and the 30 most resistant cultivars. Panel A shows a frequency histogram of ρ_{leaf} based on individual leaves from two replicates and two time points. Two insets illustrate the relationship between ρ_{leaf} and AUDPC with respect to means (panel F) and medians (panel E). Panels A and B extend only up to 80 along the x-axis, missing 223 data points with values between 80 and 301.

bioRxiv preprint doi: https://doi.org/10.1101/129353; this version posted April 29, 2017. The copyright holder for this preprint (which was not certified by peer review) is the author/funder, who has granted bioRxiv a license to display the preprint in perpetuity. It is made available under aCC-BY 4.0 International license.

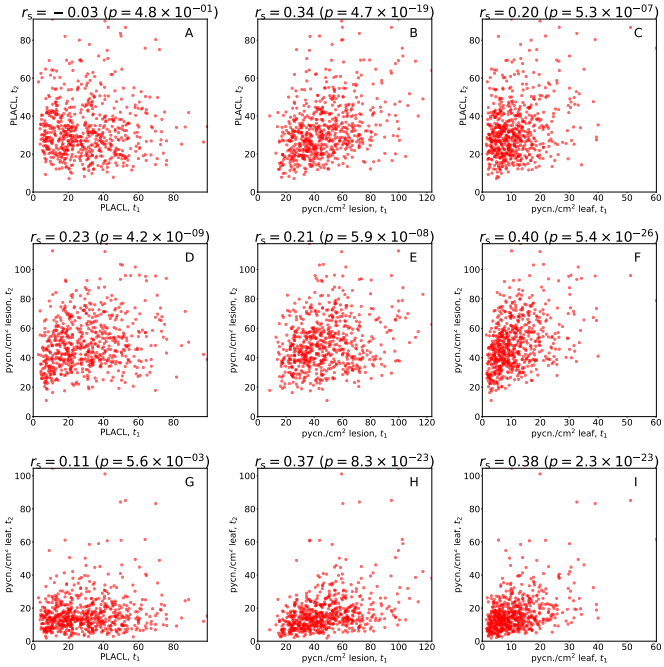

Figure 4: Correlations of measures of quantitative STB resistance between the first time point (t_1) and the second time point (t_2). The degree of correlation was quantified using Spearman's correlation coefficient, r_s. Each data point represents an average over about 16 leaves within an individual plot.

reproduction) in t_1.

Figure 4 gives a general account of the correlations/predictive power among the measured quantities in t_1 and t_2. We investigate more subtle patterns of this comparison in supplemental File S4, where we separate the effect of cultivar differences from the overall effect.

Increase of resistance to STB between t_1 and t_2. Next we investigate the difference between t_1 and t_2 to identify cultivars that exhibit an increase in resistance over time. We will refer to this as "late-onset" resistance. Each of the quantities, PLACL, ρ_{lesion} and ρ_{leaf}, increased on average between the two time points (Fig. 5). The difference was somewhat larger for ρ_{leaf} than for PLACL and ρ_{leason}. The overall mean differences are smaller than the variance of differences in individual cultivars. This is because positive changes in some cultivars were compensated by negative changes in other cultivars (as seen in Fig. 5).

We investigated the negative changes in more detail. We identified 65 cultivars in total that exhibited significant negative changes with respect to at least one of the quantities: PLACL, ρ_{lesion} or ρ_{leaf} (marked in red in Fig. 5). We see from the Venn diagram in Fig. 5D that the number of cultivars showing significant negative change in PLACL (27 cultivars) is about the same as in ρ_{lesion} (26 cultivars). None of the cultivars showed significant negative change with respect to ρ_{leaf}. The number of cultivars exhibiting

bioRxiv preprint doi: https://doi.org/10.1101/129353; this version posted April 29, 2017. The copyright holder for this preprint (which was not certified by peer review) is the author/funder, who has granted bioRxiv a license to display the preprint in perpetuity. It is made available under aCC-BY 4.0 International license.

significant negative change in terms of only one quantity were: 24 for ρ_{lesion}, 29 for PLACL. Interestingly, none of the cultivars exhibited significant negative change for both PLACL and ρ_{lesion}. PLACL decreased most in cultivars Achat and Mewa (by 54 and 41 units, correspondingly). ρ_{lesion} decreased most in cultivars Bogatka and Lindos (by about 45 units in both cases). ρ_{leaf} decreased most in cultivars Cetus and Zyta (by 19 and 15 units, correspondingly). Lists of cultivars with the corresponding magnitudes of changes are given in supplemental Tables S8–10.

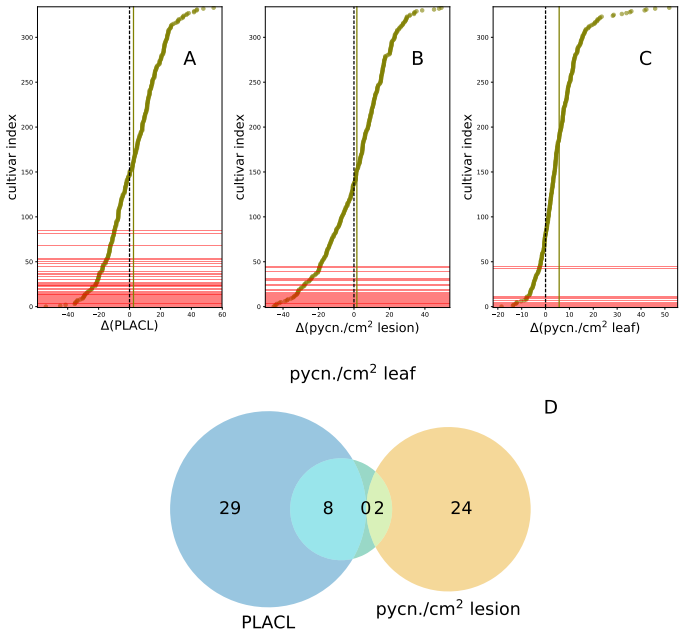

Figure 5: Indications for late-onset resistance. x-axes of plots show differences between mean values at time point t_2 and time point t_1 for the three quantities (yellow markers): PLACL (panel A), ρ_{lesion} (panel B) and ρ_{leaf} (panel C). y-axes represent cultivar indices; cultivars are sorted in order of increasing differences. Solid vertical lines show differences averaged over all cultivars; dashed vertical lines show zero differences. Cultivars exhibiting significant negative differences (according to Wilcoxon rank sum test with the FDR correction, $p < 0.01$) are shown in red. Panel D depicts a Venn diagram of cultivars with significant negative differences with respect to the three measures of resistance.

Discussion

Novel aspects of the experimental design Although fungicides suppressed STB development as compared to untreated plots, the most important benefit of the fungicide applications in the context of this experiment was to eliminate competing diseases (rusts, powdery mildews, tan spot) that usually co-exist with STB in naturally infected fields. This resulted in a nearly pure culture of STB across both replications. Virtually every

bioRxiv preprint doi: https://doi.org/10.1101/129353; this version posted April 29, 2017. The copyright holder for this preprint (which was not certified by peer review) is the author/funder, who has granted bioRxiv a license to display the preprint in perpetuity. It is made available under aCC-BY 4.0 International license.

disease lesion found on a leaf was shown to be the result of an infection by *Z. tritici*. The widespread STB infection found in this experiment could be explained by the weather during the 2015-2016 growing season that was highly conducive to development of STB (cool and wet) coupled with a significant amount of resistance to azoles in European populations of *Z. tritici* (Brunner et al., 2008).

This experimental design provided an unusual opportunity to directly compare levels and development of STB infection and STB resistance across a broad cross-section of elite European winter wheat cultivars. Combined with the novel automated image analysis method, this allowed us to collect a large amount of high-quality data with a relatively low workload.

The measures of resistance that we characterized here, on average, represent "general" or "field" resistance because the experiment was conducted using natural infection in a year that was highly conducive to STB. Cultivars that were highly resistant under these conditions are likely to be broadly resistant to the typically genetically diverse *Z. tritici* populations (Linde et al., 2002; Zhan et al., 2003).

Comparison between datasets obtained from automated image analysis and visual scoring. Conventional visual assessment typically quantifies leaf necrosis (host damage) caused by the pathogen by integrating disease severity (as PLACL) and incidence (as the proportion of leaves having necrotic lesions) into a single index. Pycnidia (an indicator of pathogen reproduction) are typically considered as a presence/absence qualitative trait that helps to separate STB from other leaf diseases. The conventional visual assessment is fast: only about nine hours in total were needed to assess more than 700 small plots three times during the season by a single person (i. e., about three hours at each measurement date).

Visual scoring benefits from a large sample size, as almost all leaves in a plot are considered compared to only 16 leaves used for image analysis. However, due to a subjective nature of the conventional scoring process, the sample size used is not clearly defined and we could not obtain statistically significant differences between cultivars based on visual scoring. Moreover, assessment of changes in traits between two timepoints is almost impossible. Uncertainty in detection of pycnidia in the conventional measurement may even lead to misestimation of resistance. Overestimation may result on cultivars that are susceptible to host damage (have high PLACL) but suppress pathogen reproduction (have low ρ_{lesion}), because failure to detect pycnidia may be interpreted as absence of the pathogen. On the other hand, if visual assessment finds pycnidia (scored as present or absent), the resistance of a cultivar may be underestimated if the degree of suppression of pycnidia production is not considered.

In contrast, automated analysis of individual leaves enables independent measurement of different forms of disease conditional severity, i.e. the degree to which infected leaves are affected by disease. The advantage of the automated method based on leaf images is that it accounts for both host damage and pathogen reproduction in a reproducible, quantitative way with a well-defined sample size. This alleviates the uncertainty in detecting pycnidia and also allowed us to find statistically significant differences be-

bioRxiv preprint doi: https://doi.org/10.1101/129353; this version posted April 29, 2017. The copyright holder for this preprint (which was not certified by peer review) is the author/funder, who has granted bioRxiv a license to display the preprint in perpetuity. It is made available under aCC-BY 4.0 International license.

tween cultivars. But this method does not consider disease incidence and is more labor-intensive than visual scoring. About 360 person-hours were needed to collect and process 21551 leaves and obtain raw data. Although this is an automated method, one needs to carefully determine its error rate at every use (as for example we described above in the "Materials and Methods" section), because errors may be cultivar-specific and also depend on environmental conditions.

Manual generation of this large dataset that included more than five million pycnidia would not be practical. However, we demonstrated that combining cheap scanners with public domain software to conduct automatic image analysis makes it feasible to separate different components of quantitative host resistance.

Host damage vs. pathogen reproduction. Biologically, PLACL reflects the pathogen's ability to invade and damage (necrotize) the host leaf tissue, while ρ_{lesion} reflects the pathogen's ability to convert the damaged host tissue into reproductive structures and eventually into offspring. From the host's perspective, PLACL can be interpreted as the degree of susceptibility to damage caused by the pathogen itself (e. g., through secretion of phytotoxins) or by host defense reactions (e. g., the hypersensitive response) activated after detecting the pathogen. ρ_{lesion} can be interpreted as measuring the host's ability to suppress pathogen reproduction, a more susceptible host enables more pathogen reproduction per unit of infected leaf area. Automated image analysis enabled us to differentiate between host damage and pathogen reproduction and hence to measure these as separate components of STB resistance.

The phenotypic differences observed in our experiment may reflect different sets of resistance genes underlying these two traits. We hypothesize that PLACL reflects additive actions of toxin sensitivity genes carried by different wheat cultivars that interact with host-specific toxins produced by the pathogen, as shown for Parastagonospora nodorum on wheat (e. g. Friesen et al., 2008; Oliver et al., 2012). We hypothesize that pycnidia density reflects additive actions of quantitative resistance genes that recognize pathogen effectors (e.g. AvrStb6 recognized by Stb6; Zhong et al. (2017, in press)) and activate plant defenses in a quantitative way (Krattinger et al., 2009). We anticipate testing these hypotheses by combining the phenotypic data reported here with wheat genome data (Marcussen et al., 2014) to conduct a genome-wide association study (GWAS) aiming to identify chromosomal regions and candidate genes underlying both components of quantitative resistance.

The density of pycnidia per unit leaf area, ρ_{leaf}, is a measure of infection that incorporates both host damage and pathogen reproduction, reflecting the pathogen's overall ability to convert healthy host tissue into reproductive units that can drive a new cycle of infection. The complex nature of quantitative host-pathogen interactions may lead to high PLACL combined with low ρ_{lesion} or low PLACL combined with high ρ_{lesion}. In both of these cases, the infection is less severe than when an interaction leads to a high ρ_{leaf}. Therefore, we believe that ρ_{leaf} better characterizes overall host resistance, pathogen fitness and STB severity than PLACL or ρ_{lesion}.

bioRxiv preprint doi: https://doi.org/10.1101/129353; this version posted April 29, 2017. The copyright holder for this preprint (which was not certified by peer review) is the author/funder, who has granted bioRxiv a license to display the preprint in perpetuity. It is made available under aCC-BY 4.0 International license.

Ranking of cultivars. The overall differences among cultivars were relatively small, except for a small number of cultivars at each extreme. These small differences are reflected in the limited number of significantly different groups of cultivars. However, our analyses showed that ranking of cultivars differs considerably with respect to the two components of quantitative resistance: resistance to host damage and resistance to pathogen reproduction (Fig. 2D). More specifically, we identified cultivars that strongly exhibit one component, while the other component is virtually absent (points in upper-left and lower-right corners of Fig. 2F). We expect that resistance that lowers pycnidia production will have greater overall impact on reducing damaging STB epidemics because it will reduce the rate of epidemic increase more than resistance to host damage. Conventional phenotyping technology based on visual assessment does not enable separation of these different components of resistance.

We expected that conventional visual assessment (based on AUDPC) would correlate best with the measurement of host damage (PLACL), as conventional assessment consists mainly of quantifying leaf necrosis, but uses pycnidia mainly qualitatively to confirm the presence of STB. Surprisingly, the measure that combines host damage and pathogen reproduction (ρ_{leaf}) gave the best correlation with the conventional assessment (cf. Figs. 3, E2.3 and E2.4). A possible explanation for this high correlation is that the conventional assessment may actually quantify pycnidia, but in a subjective way. An alternative explanation is that because conventional assessment includes both disease severity and incidence, it captures the overall pathogen population size that depends on both host damage and pathogen reproduction.

Correlation between our combined measure (ρ_{leaf}) and the conventional measure (AUDPC) in Fig. 3 indicates that breeding may have selected for cultivars that combine resistance to host damage and resistance to pathogen reproduction. This hypothesis is supported by the small but significant positive correlations between PLACL and ρ_{lesion} in terms of both means and medians over individual cultivars (Fig. 2F).

Interestingly, the same two quantities, PLACL and ρ_{lesion} show a negative correlation when analyzed at the level of individual leaves (Fig. 2G). Comparisons of means/medians based on many leaves from the same cultivar shows the effect of the cultivar on the relationship between PLACL and ρ_{lesion}. (See Appendix A.4 for discussion on the use of means vs. medians in the analysis). Comparisons based on individual leaves take into account both the cultivar effect and the pathogen effect on each leaf. The negative correlation in the individual leaf data may indicate a pathogen-level tradeoff between PLACL and ρ_{lesion}. This tradeoff may have a genetic basis as an epistatic interaction between the two components of quantitative resistance described above. It may also reflect a resource allocation tradeoff between invasion of host tissue and production of pycnidia. *Z. tritici* isolates sampled from the two extremes of the hypothetical tradeoff could be used for phenotypic confirmation of strain specific PLACL-ρ_{leaf} -relationship as well as for identification of the genetic basis of these traits. To detect strain-specific differences in PLACL between different pathogen strains in a greenhouse experiment, concentration of spores in the inoculum will need to be lower than typically used (to insure that PLACL is lower than 100 %).

bioRxiv preprint doi: https://doi.org/10.1101/129353; this version posted April 29, 2017. The copyright holder for this preprint (which was not certified by peer review) is the author/funder, who has granted bioRxiv a license to display the preprint in perpetuity. It is made available under aCC-BY 4.0 International license.

Predictors of epidemic development. PLACL on upper leaves is a key determinant of disease-induced yield loss (e.g., Brokenshire, 1976). Hence, the ability to predict PLACL on the upper leaves late in the growing season based on an early season measurement may improve disease control. Our results suggest this possibility: the measure that quantifies pathogen reproduction, ρ_{lesion}, evaluated early in the season (at t_1, approximately GS 41) predicts the late-season host damage (PLACL at t_2, approximately GS 75-85) better than early-season PLACL or ρ_{leaf} (see Fig. 4, compare panel B with panels A and C). We postulate that this finding could improve decision-making for fungicide application: one may decide to apply fungicides only if ρ_{lesion} exceeds a certain threshold early in the season.

Increase of resistance to STB between t_1 and t_2. Negative changes with respect to quantities characterizing host susceptibility (PLACL, ρ_{lesion}, and ρ_{leaf}) suggest an increase in host resistance over time. We found that none of the cultivars exhibited this property in terms of both PLACL, ρ_{lesion}. Accordingly, none of them showed a significant decrease only in the combined measure, ρ_{leaf}, and not in any other measure. This may indicate that the genetic basis of the late-onset resistance differs between host damage and pathogen reproduction. These outcomes may help to reveal the genetic basis of "late-onset" resistance to STB (e.g. using GWAS or QTL mapping).

The degree of resistance or the intensity of a development can only be assessed from multiple, quantitative measurements at subsequent points in time. Such dynamically developing traits require an objective evaluation and cannot be assessed by visual grading. This is one of the most important advantages of imaging-based phenotyping methods compared to classical grading-based phenotyping (Walter et al., 2015; Kirchgessner et al., 2017)

Conclusions. We utilized a novel phenotyping technology based on automated analysis of digital leaf images to compare quantitative resistance to STB in 335 European wheat cultivars naturally infected by a highly variable local population of *Z. tritici*. This method allowed us to distinguish between resistance components affecting host damage (PLACL) and resistance components affecting pathogen reproduction (lesion pycnidia density and pycnidia size). Measurements of pycnidia density cannot be accomplished on such a large scale with traditional assessment methods and may provide a new and powerful tool for measuring quantitative resistance to STB.

To our knowledge this is the most comprehensive characterisation of the two components of resistance separately. As suggested by Simko et al. (2017), digital phenotyping reduces subjectivity in trait quantification. Thus the present method may reveal small differences that wouldn't be observed without. Development of the method could involve adjustment of the analysis parameters to be suitable for each cultivar separately, machine learning for more precise detection of symptoms and combining it with incidence data gathered for example by image analysis of high-quality canopy images such as produced by the phenomobile (Deery et al., 2014) or the ETH field phenotyping platform (Kirchgessner et al., 2017).

bioRxiv preprint doi: https://doi.org/10.1101/129353; this version posted April 29, 2017. The copyright holder for this preprint (which was not certified by peer review) is the author/funder, who has granted bioRxiv a license to display the preprint in perpetuity. It is made available under aCC-BY 4.0 International license.

Outlook. Our approach can be readily applied to classical phenotype-based selection and breeding. Cultivars that show high resistance to both host damage and pathogen reproduction will be most likely to strongly suppress the pathogen population at the field level and result in less overall damage due to STB. Importantly, cultivars that show the highest resistance based on either host damage or pathogen reproduction can be used in breeding programs as independent sources of these two components of resistance. An important novelty of our approach is provide a powerful method to specifically breed wheat cultivars carrying resistance that suppresses pathogen reproduction.

While the ability to separate phenotypes associated with two different aspects of resistance provides new avenues for resistance breeding, our hypothesis that the two components of resistance are under separate genetic control remains to be confirmed by further research. We anticipate that future genetic studies (e.g. using GWAS) based on these phenotypic data will enable us to identify genetic markers that are linked to the different types of resistance. These markers could then enable joint selection of the different forms of resistance via marker-assisted breeding or in a genomic selection pipeline. If we can validate our hypothesis that toxin sensitivity genes underlie differences in PLACL among cultivars, the breeding objective would be to remove these sensitivity genes (Friesen et al., 2008; Oliver et al., 2012).

Acknowledgements

PK and AM gratefully acknowledge financial support from the Swiss National Science Foundation through the Ambizione grant PZOOP3_161453 "Epidemiology of major wheat diseases: using eco-evolutionary models to learn from epidemic and genomic data". The authors are grateful to Danilo Dos Santos Pereira, Simone Fouche and Lukas Meile for help in collecting and processing leaf samples, to Ethan Stewart for advice and guidance in using the leaf image analysis software, and to Hansueli Zellweger for managing the wheat trial.

A. Appendix

A.1. Estimation of the number of pathogen generations

We estimated the number of asexual cycles of pathogen reproduction (number of generations) using data on the dependency of the latent period of *Z. tritici* on temperature [Fig. 5 in (Shaw, 1990)]. We are interested in the overall relationship between the latent period and the temperature and would like to use the largest amount of data available. For this reason, we pooled together the data available for two cultivars, Avalon and Longbow, recorded by Shaw (1990). Next, we fitted the polynomial function

$$1/\Delta t_l = a\theta - b\theta^4 \tag{A.1}$$

bioRxiv preprint doi: https://doi.org/10.1101/129353; this version posted April 29, 2017. The copyright holder for this preprint (which was not certified by peer review) is the author/funder, who has granted bioRxiv a license to display the preprint in perpetuity. It is made available under aCC-BY 4.0 International license.

to the resulting data. Here, Δt_l is the latent period, θ is the temperature, a and b are fitting parameters. The outcome is shown in Fig. A1. Best-fit values of parameters are:

$$a = (4.5 \pm 0.6) \times 10^{-3},\ b = (3.9 \pm 1.0) \times 10^{-7}. \tag{A.2}$$

Uncertainties in Eq. A.2 represent the 95 % confidence intervals calculated from standard errors. Goodness of fit: $R^2 = 0.7$; standard error of regression $s = 5.5 \times 10^{-3}$.

We then used average daily temperatures and amount of rainfall measured at the Lindau weather station located close to our experimental site to estimate the number of pathogen generations, n_g. We performed estimation of n_g per growing season (from March 1 until July 27) and between two sampling dates (from May 1 until July 4). First, we determined the average latent period from the daily temperature averaged over the growing season using Eq. A.1 with the parameter values Eq. A.2. This resulted in the value $\Delta t_l = 21$ days. After that we introduced a constraint on the number of pathogen generations using the rainfall data. According to our current understanding, rainfall is the most efficient way to release and disperse the asexual pycnidiospores. For this reason, we assumed that a cycle of asexual reproduction could only be completed after a day with at least 5 mm rainfall [similar to (Zhan et al., 2002)]. In this way we estimated an average of about six cycles of asexual reproduction during the growing season and about two cycles between the two sampling dates t_1 and t_2 (Fig. A2).

bioRxiv preprint doi: https://doi.org/10.1101/129353; this version posted April 29, 2017. The copyright holder for this preprint (which was not certified by peer review) is the author/funder, who has granted bioRxiv a license to display the preprint in perpetuity. It is made available under aCC-BY 4.0 International license.

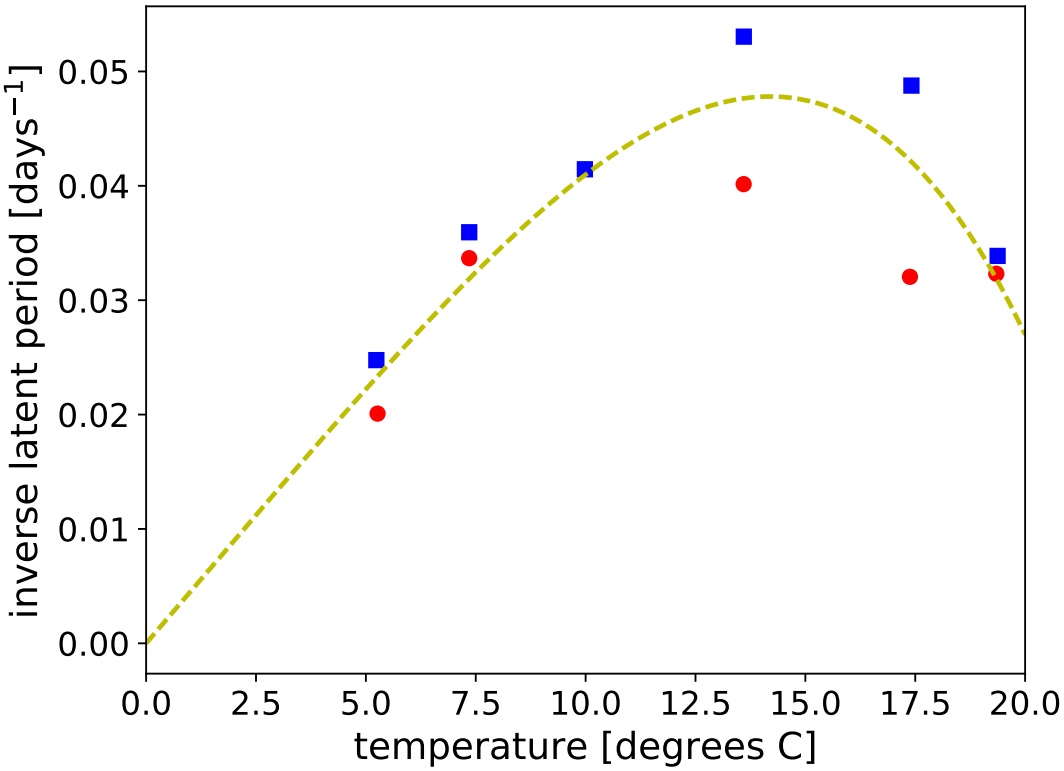

Figure A1: Inverse of latent period of *Z. tritici* as a function of the temperature, data from Fig. 5 (Shaw, 1990). Data from controlled-environment experiments for cultivars Longbow (circles) and Avalon (squares). Dashed curve is the best fit using the function in Eq. A.1 (see text for details).

bioRxiv preprint doi: https://doi.org/10.1101/129353; this version posted April 29, 2017. The copyright holder for this preprint (which was not certified by peer review) is the author/funder, who has granted bioRxiv a license to display the preprint in perpetuity. It is made available under aCC-BY 4.0 International license.

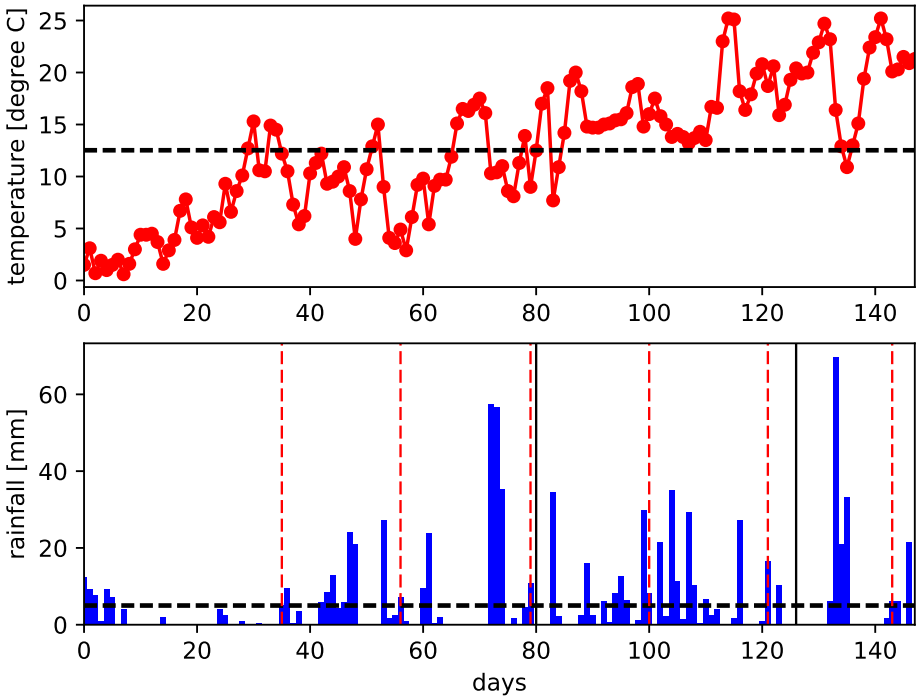

Figure A2: Temperature and rainfall data recorded at the Lindau weather station (data from http://www.agrometeo.ch/de/meteorology/datas) for the period between March 1 and July 27, 2016. Red vertical lines indicates the generation times and black vertical times show the sampling dates t_1 and t_2.

A.2. Calculation of AUDPC based on visual assessments

We denote the values of visual scores recorded on the first, τ_1, second, τ_2 and third, τ_3, dates (20th of May, 21th of June and 29th of June, 2016) of visual assessments as A_1, A_2 and A_3. Area under the disease progress curve (AUDPC) was calculated for each cultivar using the visual scores in the following manner:

$$\text{AUDPC} = \frac{1}{2}\left(\tau_2 A_1 + (\tau_3 - \tau_1)A_2 + (\tau_3 - \tau_2)A_3\right), \tag{A.3}$$

where $\tau_1 = 14\,\text{days}$, $\tau_2 = 44\,\text{days}$, $\tau_3 = 52\,\text{days}$. Here, we assumed that disease started from zero 14 days before the first scoring, values of A_1, A_2 and A_3 are taken as average scores over two replicate plots. Eq. A.3 uses a trapezoidal function to interpolate between the time points in order to calculate the area under the curve. This assumes that score values are connected by linear segments. Values of AUPDC are shown for each cultivar in Fig. 3D of the main text.

To analyze differences between cultivars, we weighted scores A_1, A_2 and A_3 in the following manner: $a_1 = 3\tau_2 A_1/2$, $a_2 = 3(\tau_3 - \tau_1)A_2/2$, $a_3 = 3(\tau_3 - \tau_2)A_3/2$. The

bioRxiv preprint doi: https://doi.org/10.1101/129353; this version posted April 29, 2017. The copyright holder for this preprint (which was not certified by peer review) is the author/funder, who has granted bioRxiv a license to display the preprint in perpetuity. It is made available under aCC-BY 4.0 International license.

coefficients were chosen such that weighted scores a_1, a_2 and a_3 give proportionate contribution to the AUDPC and the arithmetic average over them gives the AUDPC. The weighted scores from each replicate and each time point were given as a set of points corresponding to each cultivars (total of six measurement points per cultivar). One score was missing for one of the replicates in several cultivars. For these cultivars, we used only five measurement points for statistical analysis. We also calculated grand means over raw (not weighted) visual scores for each cultivar by taking arithmetic means over measurements in two replicates and three time points (six measurement points). Similarly to the case of weighted scores, when scores were missing in one of replicates at one of time points, we calculated arithmetic means over the five values that were present.

Statistical differences between cultivars based on visual scoring could, in principle, be tested with a similar manner as based on image analysis data. We tested differences between distributions based on weighted visual scores of cultivars. The global Kruskal-Wallis test (R Core Team, 2016) revealed no differences (Kruskal-Wallis chi-squared = 194.39, df = 335, $p = 1$). Surprisingly, when using unweighted visual scores there were differences between cultivars (Kruskal-Wallis chi-squared = 642.4, df = 335, $p < 2.2 \cdot 10^{-16}$). Pairwise multiple comparison with a false discovery rate p-value correction (Benjamini and Hochberg, 1995) found out that the 23 most susceptible cultivars were different from the most resistant and the 155 most resistant cultivars were different from the most susceptible. However, there were 158 cultivars that were not significantly different from either extreme. The slight but significant difference between unweighted and weighted data may arise from the short time interval between τ_2 and τ_3. Thus cultivars cannot be distinguished by weighted scores, as the last scoring time, resulting likely in the greatest differences between visual scorings of cultivars, had the smallest effect on AUDPC and consequently differences arising from latest scores are suppressed.

Despite differences between statistical properties of unweighted and weighted data, the ranking based on them is pretty similar: Spearman's correlation between mean ranks of unweighted and weighted scores of cultivars is high ($r_s = 0.97$, $p < 2.2 \cdot 10^{-16}$). Also Spearman's correlations between AUDPC, mean rank of unweighted scores and arithmetic mean of unweighted scores are high (AUDPC vs. mean ranks: $r_s = 0.97$; AUDPC vs. means: $r_s = 0.97$; mean ranks vs means $r_s = 0.998$; $p < 2.2 \cdot 10^{-16}$ for each).

A.3. Correlation between replicates

Correlations between the biological replicates ranged from 0.3 to 0.7 (Fig. A3). The highest correlation between the two replicates was found in pycnidia grey value at t_1. The lowest correlation was in PLACL at t_1. PLACL showed the largest difference in correlation coefficients between replicates. The exceptionally low correlation between replicates at t_1 for PLACL and necrotic area may have arisen from making the collection at a critical point in the epidemic: if the last infection cycle had been just entering the necrotic phase (as suggested in Fig. A2), there could have been huge variation between replicates by chance due to the highly variable length of the latent period for STB

bioRxiv preprint doi: https://doi.org/10.1101/129353; this version posted April 29, 2017. The copyright holder for this preprint (which was not certified by peer review) is the author/funder, who has granted bioRxiv a license to display the preprint in perpetuity. It is made available under aCC-BY 4.0 International license.

infection.

Spearman's correlation describes linear relationship between rankings based on the two replicates. Moderate but highly significant correlations between replicates for each measure imply that resistance rankings based on these measures may differ considerably between replicates. We expect this to result from the shape of the quantitative resistance distributions (Fig. 2 and 3 of the main text). For all three main measures of resistance, PLACL, ρ_{lesion} and ρ_{leaf}, means of the measure are quite similar for all cultivars except a small number of cultivars at the phenotype extremes. Thus even a little variation in these measures between replicates may result in a large change in ranking of the cultivar for one replicate to other. This is also implied by the small statistical differences between cultivars in the middle of the distributions (Fig. 2 and 3 of the main text).

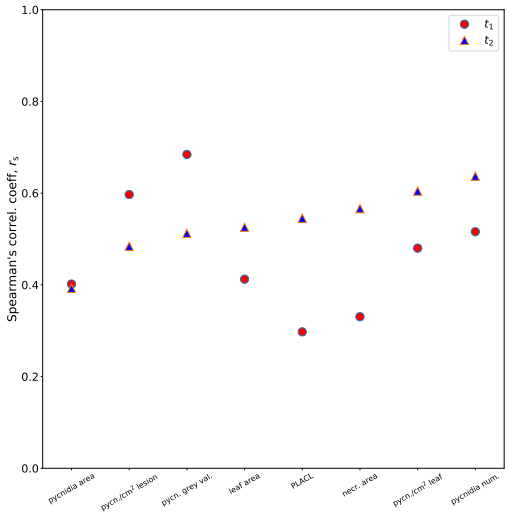

Figure A3: Spearman's correlation coefficient between the mean values (taken over leaves belonging to the same cultivar) in two replicates for eight different quantities. All results are highly significant ($p < 10^{-7}$).

A.4. The use of means vs. medians in the analysis of STB resistance

As our data was clearly non-normal, the central tendency of the data may be better described by medians than means. Comparing medians is also biologically reasonable: total yield is more likely determined by a large number of moderately damaged wheat plants, than by the few fully diseased or dead plants. We also found stronger correlation between AUDPC and medians of PLACL and ρ_{lesion} than AUDPC and means of PLACL and ρ_{lesion}. Nevertheless, when comparing AUDPC and ρ_{leaf} we found stronger correlation between AUDPC and means of ρ_{leaf} than medians. This may indicate that mean values better describe the way breeders traditionally assessed diseases caused by

bioRxiv preprint doi: https://doi.org/10.1101/129353; this version posted April 29, 2017. The copyright holder for this preprint (which was not certified by peer review) is the author/funder, who has granted bioRxiv a license to display the preprint in perpetuity. It is made available under aCC-BY 4.0 International license.

necrotrophs. If this insight proves true, it may help us understand and counteract the subjective nature of visual assessment with its tendency to overweight fully diseased plants and overestimate the overall severity.

E. eXtra

E1. Description of eXtra tables and figures

Supplemental File S1 presents the list Supplemental File S1 describes content of each supplemental file and table. Supplemental File S2 shows full range versions of ranking figures (Figs. 2 and 3 of the main text) and also additional comparisons between PLACL and ρ_{leaf}, PLACL and AUDPC, and ρ_{lesion} and AUDPC. Supplemental File S3 shows comparison between means, medians and mean ranks of PLACL, ρ_{lesion}, and ρ_{leaf}. Supplemental File S4 shows detailed analysis af predictive power of PLACL, ρ_{lesion}, and ρ_{leaf} at t_1 on those variables at t_2 and considers separately "cultivar effect" and "pathogen effect".

Supplemental Table S1 provides the parameter values used in the ImageJ macro and can be used directly as the input to the macro.

Supplemental tables supporting Fig. 2 and Fig. 3 of the main text display information on ranking of cultivars in tab-delimited text files. Supplemental Tables S2, S3 and S4 show cultivar names in first column; genetic identification number in second column; mean of observable (PLACL, ρ_{lesion}, ρ_{leaf}; respectively) over all the leaves of a cultivar in the third colum; standard error of the mean in the fourth column and median in the fifth column. The tables are sorted according to descending mean. In Supplemental Tables S5–S7 cultivars are ranked according to mean rank of leaves of a cultivar according to corresponding measurement. First column shows cultivar names; second genetic id; third mean rank of the data and fourth grouping code, regarding statistical differences between cultivars according to multiple pairwise Kruskal-Wallis comparison with false discovery rate p-value correction (cultivars having same letter in the grouping code are not significantly different). The tables are sorted according to descending mean rank. All tables contain a header row naming the columns.

Supplemental Tables S8–S10 supporting Fig. 5 of the main text display information on cultivars that exhibit significant negative change between t_1 and t_2 in mean values of PLACL, ρ_{lesion} and ρ_{leaf}, respectively. Cultivars are sorted according to the difference between the mean values in t_1 and t_2. First column shows cultivar names; second column shows mean values in t_1; third column shows mean values t_2; fourth columns shows the difference between means in t_1 and t_2; fifth col: W statistic of the Wilcoxon rank sum test; 6th col: p-value of the Wilcoxon rank sum test with FDR correction.

E2. Ranking of cultivars

In Fig. E2.1 cultivars are ranked as in Fig. 2 of the main taxt and the full range of raw data is shown for ρ_{lesion}. Significantly differing groups of cultivars are labeled with

bioRxiv preprint doi: https://doi.org/10.1101/129353; this version posted April 29, 2017. The copyright holder for this preprint (which was not certified by peer review) is the author/funder, who has granted bioRxiv a license to display the preprint in perpetuity. It is made available under aCC-BY 4.0 International license.

different colors (excluding gray). Fig. E2.2 has the same organizing principle except that Fig. E2.2E shows ranking according to ρ_{leaf}. Details of correlations are shown in insets (F, G, H) as in Fig. 2 of the main text.

In Figs. E2.3 and E2.4 the connection between traditional resistance measurement (AUDPC) and either PLACL or ρ_{lesion}, respectively, are given similarly to what was shown in Fig. 3 of the main text. Spearman's correlation coefficients are higher between medians of PLACL or ρ_{lesion} and AUDPC than between means of those and AUDPC. Details of correlations are given in the insets (E, F).

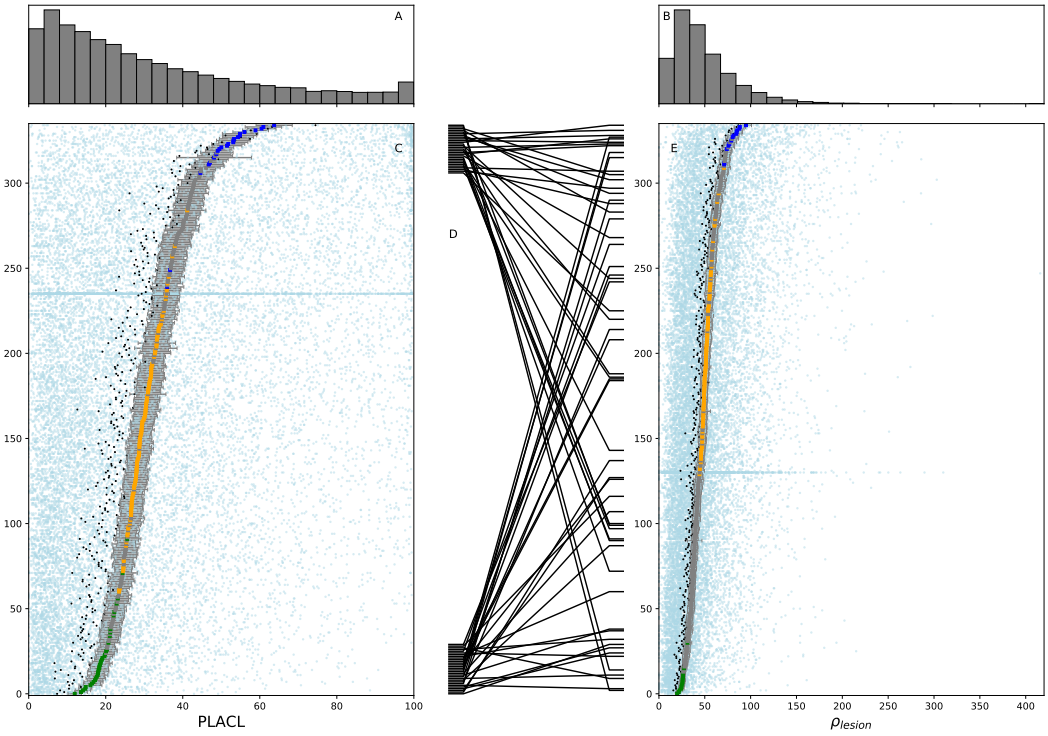

Figure E2.1: This figure is the same as Fig. 2 of the main text except that panel E shows the full range of data points of ρ_{lesion}.

bioRxiv preprint doi: https://doi.org/10.1101/129353; this version posted April 29, 2017. The copyright holder for this preprint (which was not certified by peer review) is the author/funder, who has granted bioRxiv a license to display the preprint in perpetuity. It is made available under aCC-BY 4.0 International license.

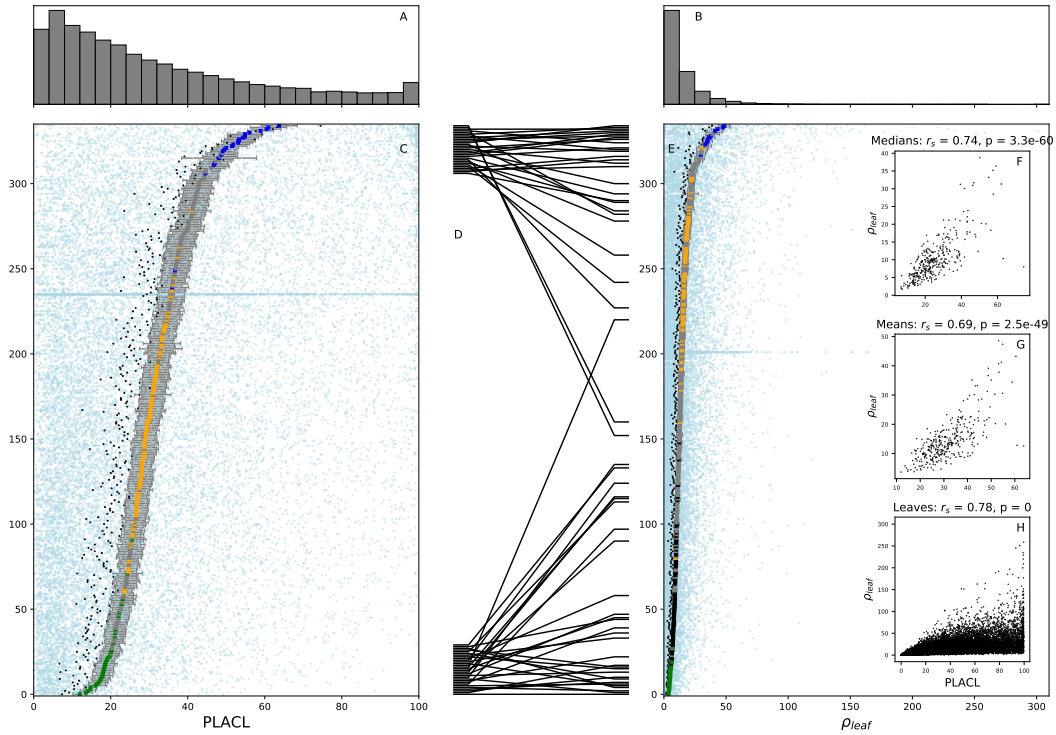

Figure E2.2: The organzation of the figure is the same as in Fig. 2 of the main text, but here panel E shows data of ρ_{leaf} and correspondingly insets F, G and H show correlations between PLACL and ρ_{leaf}.

bioRxiv preprint doi: https://doi.org/10.1101/129353; this version posted April 29, 2017. The copyright holder for this preprint (which was not certified by peer review) is the author/funder, who has granted bioRxiv a license to display the preprint in perpetuity. It is made available under aCC-BY 4.0 International license.

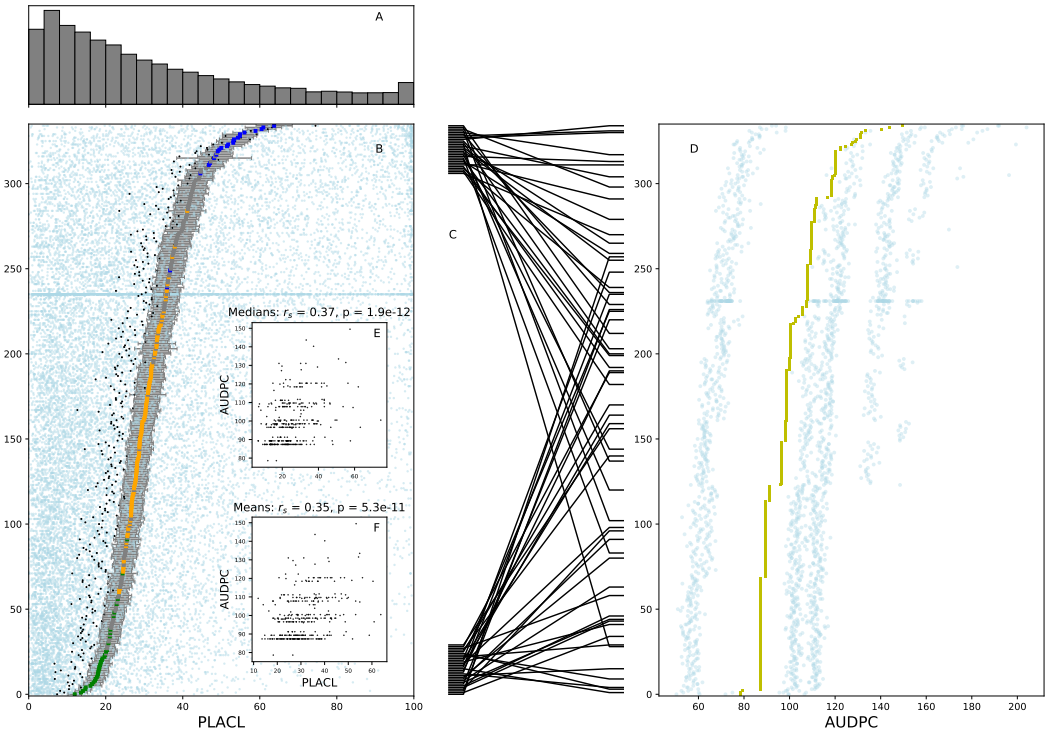

Figure E2.3: The organzation of the figure is the same as in Fig. 3 of the main text, but here panel B shows data of PLACL and correspondingly insets E and F show correlations between PLACL and AUDPC.

bioRxiv preprint doi: https://doi.org/10.1101/129353; this version posted April 29, 2017. The copyright holder for this preprint (which was not certified by peer review) is the author/funder, who has granted bioRxiv a license to display the preprint in perpetuity. It is made available under aCC-BY 4.0 International license.

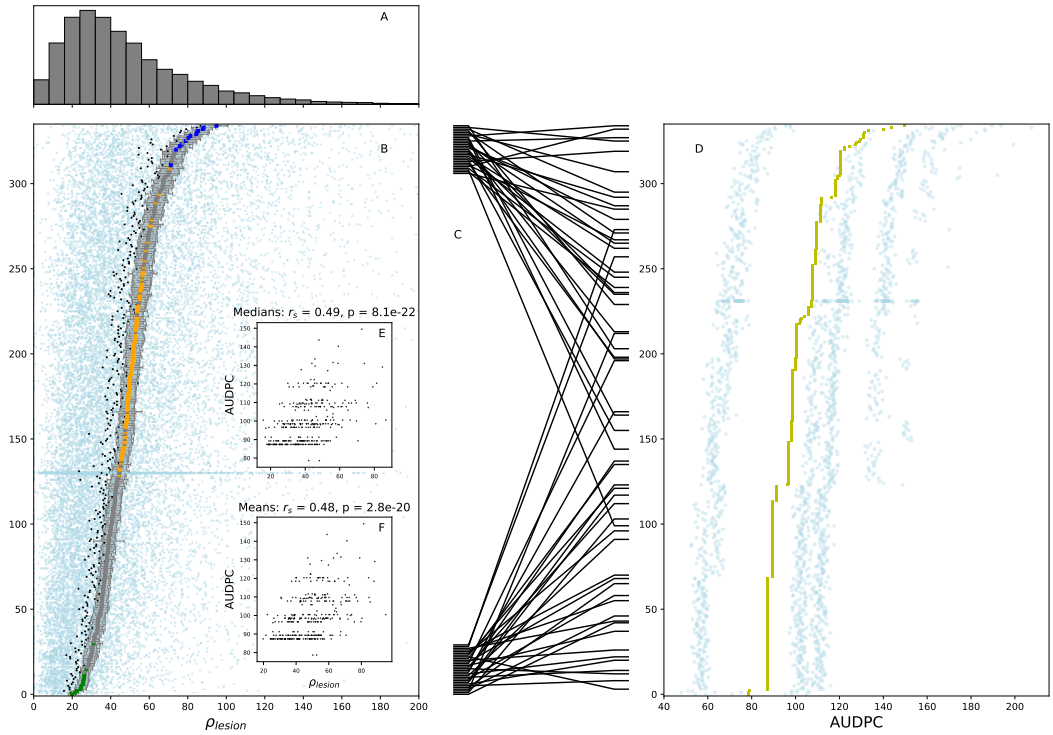

Figure E2.4: The organzation of the figure is the same as in Fig. 3 of the main text, but here panel B shows data of ρ_{lesion} and correspondingly insets E and F show correlations between ρ_{lesion} and AUDPC.

E3. Correlation between means, medians and mean rank of PLACL, ρ_{lesion} and ρ_{leaf}

Resistance ranking of cultivars according to means, medians and mean ranks (Kruskal-Wallis test statistics) for PLACL, ρ_{lesion} and ρ_{leaf} are very strongly and statistically significantly correlated ($r \geq 0.94$) (Fig. E3.1). Thus differences between mean ranks revealed by Kruskal-Wallis comparisons (cf. Fig. 2 and Fig. 3 of the main text) are correlated to differences between ranking of cultivars according to means or medians of PLACL, ρ_{lesion} and ρ_{leaf}.

bioRxiv preprint doi: https://doi.org/10.1101/129353; this version posted April 29, 2017. The copyright holder for this preprint (which was not certified by peer review) is the author/funder, who has granted bioRxiv a license to display the preprint in perpetuity. It is made available under aCC-BY 4.0 International license.

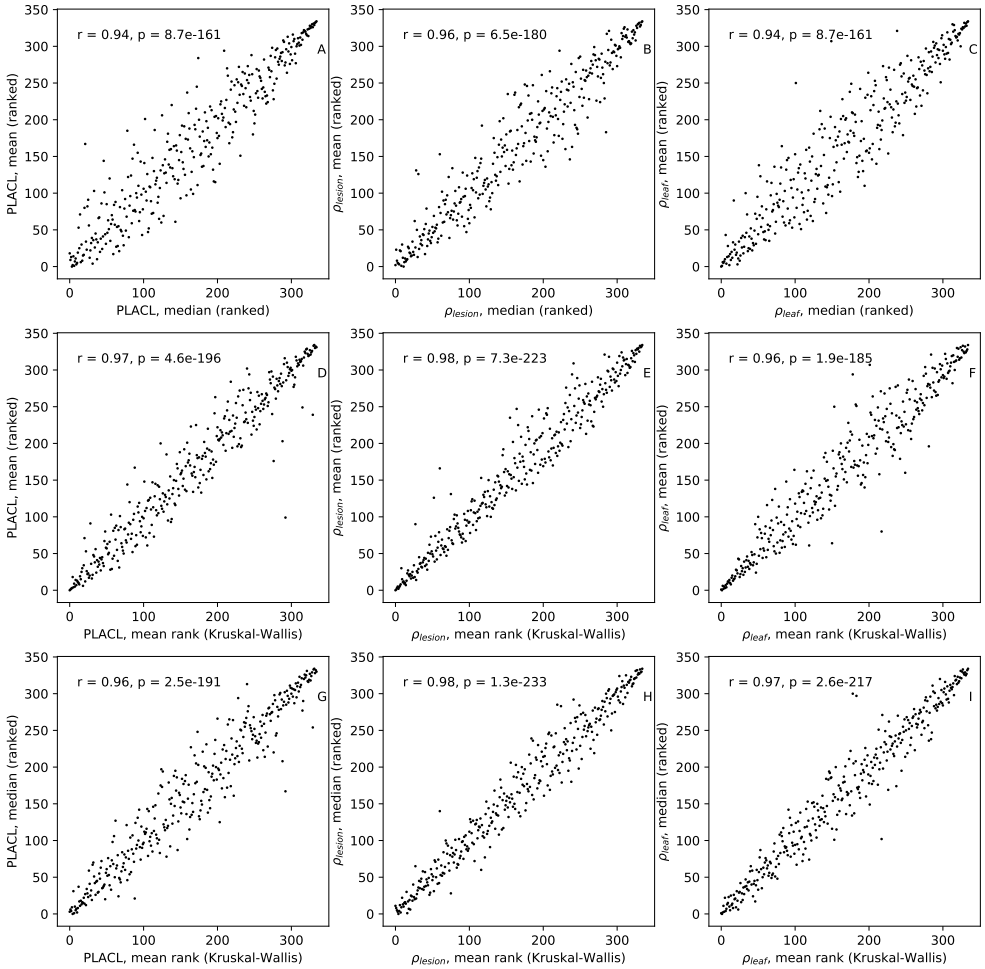

Figure E3.1: Pearson correlations between ranked means and medians and mean ranks (Kruskal-Wallis test statistics) of PLACL, ρ_{lesion} and ρ_{leaf}.

E4. Predictors of epidemic development: separating effects of cultivar and pathogen

In the section "Predictors of epidemic development" of the main text, we presented correlations between two time points for PLACL, ρ_{lesion} and ρ_{leaf} (Fig. 4 of the main text). These correlations were based on means over leaves belonging to each individual plot (with two plots per cultivar). Here, we disentangle two factors that may be responsible for the observed correlations. First is the effect of the host. In this case, the correlation is explained by differences between cultivars that remain constant over the two time

bioRxiv preprint doi: https://doi.org/10.1101/129353; this version posted April 29, 2017. The copyright holder for this preprint (which was not certified by peer review) is the author/funder, who has granted bioRxiv a license to display the preprint in perpetuity. It is made available under aCC-BY 4.0 International license.

points. For example, when cultivars that are susceptible early in the season (t_1) remain susceptible late in the season (t_2). Second, is the effect of pathogen. In this case, correlations may arise due to the highly local progression of epidemics characteristic of splash-dispersed pathogens or other cultivar-independent factors. For example, plots that had more disease early in the season would also have more disease late in the season. In other words, when considering the effect of pathogen, we investigate how well differences between plots (of the same cultivar, but located in separate lots) early in the season correlate with differences late in the season. These differences between plots may arise due to different amount of local inoculum or due to different local microenvironmental conditions. We note that genotype-environment interactions may contribute to both of these effects, but for simplicity we will refer to the two effects as "host effect" and "pathogen effect". To separate the two effects, we performed a more detailed analysis of the correlation.

To determine the effect of host, instead of using two values per cultivar that correspond to two replicate plots (as we did in Fig. 4 of the main text), we used the average of these two values for each cultivar (by averaging over about 32 leaves belonging to each cultivar at each time point, with the exception of cultivar CH Claro that had about 670 leaves per time point). We then determined correlations between these average values in t_1 and in t_2. The resulting correlations are shown in Fig. E4.1 and in columns "cv" of the Table E4.1. The highest correlation is observed between ρ_{lesion} at t_1 and ρ_{leaf} at t_2 The best predictor for late-season PLACL is ρ_{lesion} .

To determine the effect of pathogen, we normalized means over each plot in the following way. At each time point, we subtracted from each mean over plot (averaged over maximum 16 leaves) a grand mean over both plots (averaged over maximum 32 leaves) that belong to the same cultivar and time point. To balance the dominating effect of cultivar CH Claro, we used only two data points for it so that each point represents the difference between the mean over all 21 plots of CH Claro in one lot and the grand mean over 42 plots from both lots. The resulting correlations are shown in Fig. E4.2 and in columns "normed" in Table E4.1. The highest correlation is observed between PLACL at t_1 and ρ_{lesion} at t_2 The best predictor for late-season PLACL is ρ_{lesion} .

Correlations corresponding to the effect of host with respect to the same measure (PLACL, ρ_{lesion}, or ρ_{leaf}) reveal the degree to which cultivars keep their ranking according to this particular measure between t_1 and t_2 (see diagonal panels in Fig. E4.1). In these cases, correlation coefficients quantify the degree of consistency between t_1 and t_2 of host resistance to PLACL (Fig. E4.1A), ρ_{lesion} (Fig. E4.1E) and ρ_{leaf} (Fig. E4.1H). As we see from Fig. E4.1A, PLACL at t_1 has no significant correlation to PLACL at t_2. Hence, we cannot predict differences in host damage between two cultivars late in the season based on differences in host damage early in the season. Such prediction is more likely to be achieved if we considered differences between one of the most susceptible and one of the most resistant cultivars. However, when we take into account all cultivars, on average there is no significant correlation. In contrast, the correlation between ρ_{lesion} at t_1 and ρ_{lesion} at t_2 is moderately strong and highly significant ($r_s = 0.4$). We conclude that differences between cultivars according to ρ_{lesion} are more consistent than differences according to PLACL.

bioRxiv preprint doi: https://doi.org/10.1101/129353; this version posted April 29, 2017. The copyright holder for this preprint (which was not certified by peer review) is the author/funder, who has granted bioRxiv a license to display the preprint in perpetuity. It is made available under aCC-BY 4.0 International license.

Correlations corresponding to the effect of pathogen reveal the degree to which plots of the same cultivar keep their ranking between t_1 and t_2. In contrast to the "host effect" described above, PLACL at t_1 has a significant slightly negative correlation to PLACL at t_2 with respect to "pathogen effect" (Fig. E4.2A). ρ_{leaf} at t_1 and ρ_{leaf} at t_2 exhibit a moderate correlation (Fig. E4.2I). Hence, differences between plots of the same cultivar are more consistent between t_1 and t_2 with respect to ρ_{leaf} than with respect to PLACL.

To determine their relative contributions to the overall correlations shown in Fig. 4 of the main text, we compare contributions of "host effect" (Fig. E4.1) and "pathogen effect" (Fig. E4.2). Correlation between PLACL at t_1 and ρ_{lesion} at t_2 due to "pathogen effect" is positive and significant (Fig. E4.2D), while the same correlation due to cultivar effect is not significant (Fig. E4.1D). Hence, we conclude that the overall positive relationship between PLACL t_1 and ρ_{lesion} t_2 (Fig. 4D of the main text) is caused mainly by "pathogen effect". In contrast, there is no significant relationship between ρ_{lesion} at t_1 and ρ_{leaf} at t_2 due to pathogen effect (Fig. E4.2G), but there is a strong positive correlation due to "host effect" (Fig. E4.1G). This indicates that the overall positive correlation arises due to "host effect". Interestingly, ρ_{lesion} exhibits a moderate positive correlation between t_1 and t_2 due to "cultivar effect" but a negative correlation due to "pathogen effect". Reason for that phenomenon remains an open question.

Since cultivar CH Claro was replicated more than any other cultivar (a total of 42 plots), we analyzed it separately to see if the "pathogen effect" discussed above is visible in data from one cultivar. However, Spearman's correlation test did not show any significant correlation with respect to means over each of 42 plots between t_1 and t_2 for any combination of the three quantities (PLACL, ρ_{lesion} and ρ_{leaf}).

Thus, separating the "host effect" and "pathogen effect" allowed us to gain insight into the source of the correlations over time between different measures of host resistance and to better assess their predictive power. Although this analysis did not reveal extremely strong correlations, we expect, that disease forecasting models could benefit from having pathogen reproduction, not only host damage, as an explanatory variable. Combine with incidence measurements, the method presented allows for detailed quantification of pathogen population and its reproductive potential.

	PLACL(t_1)			ρ_{lesion} (t_1)			ρ_{leaf} (t_1)		
	raw	cv	normed	raw	cv	normed	raw	cv	normed
PLACL(t_2)	(-0.03)	(0.02)	-0.11	0.34	0.36	0.25	0.20	0.27	(0.022)
ρ_{lesion} (t_2)	0.23	(0.08)	0.39	0.21	0.40	-0.24	0.40	0.38	0.36
ρ_{leaf} (t_2)	0.11	(0.04)	0.23	0.37	0.49	(-0.0071)	0.38	0.40	0.29

Table E4.1: Spearman's correlations between measures of resistance in t_1 and t_2. Non-significant correlations in parentheses ($p > 0.01$). Correlations in columns "raw" are calculated using means of each plot for each time point, in columns "cv" using mean over all plots of a cultivar for each timepoint and in columns "normed" using difference of plot mean from cultivar mean for each time point as explained in the text.

bioRxiv preprint doi: https://doi.org/10.1101/129353; this version posted April 29, 2017. The copyright holder for this preprint (which was not certified by peer review) is the author/funder, who has granted bioRxiv a license to display the preprint in perpetuity. It is made available under aCC-BY 4.0 International license.

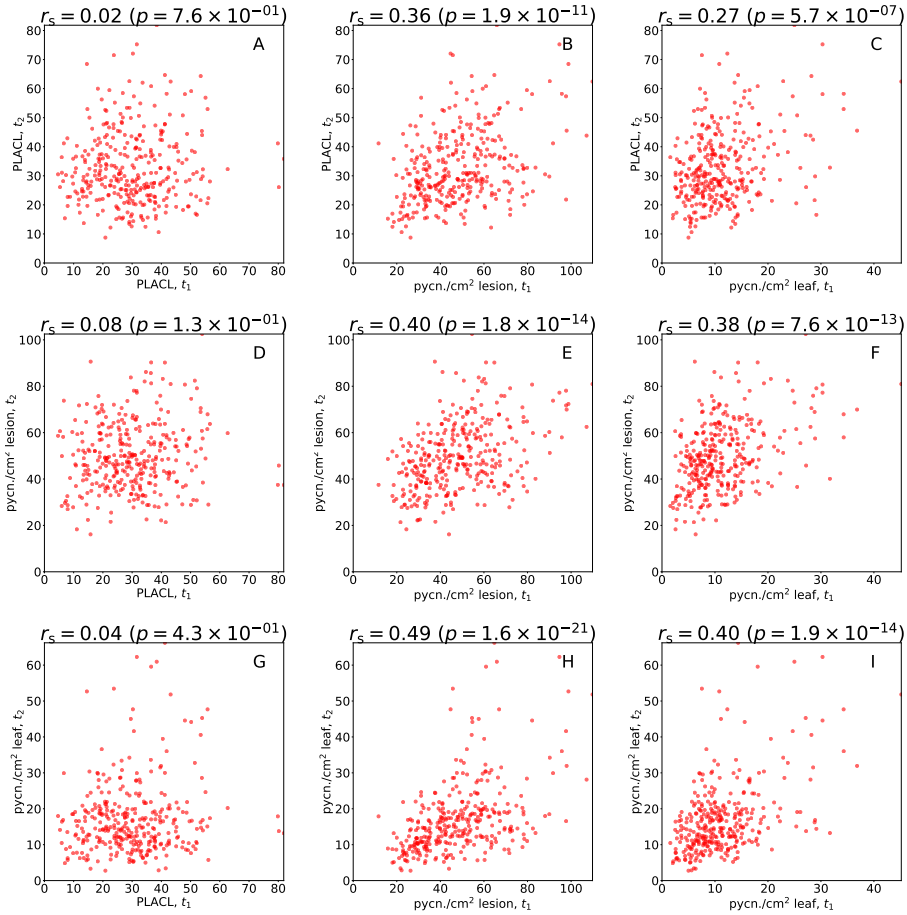

Figure E4.1: Correlation of measures of resistance (means over plots of the same cultivar) between the first time point (t_1) and the second time point (t_2). Each data point represents an average over about 32 leaves of one cultivar belonging to two replicates plots. Degree of correlation is quantified using Spearman's correlation coefficient, r_s.

bioRxiv preprint doi: https://doi.org/10.1101/129353; this version posted April 29, 2017. The copyright holder for this preprint (which was not certified by peer review) is the author/funder, who has granted bioRxiv a license to display the preprint in perpetuity. It is made available under aCC-BY 4.0 International license.

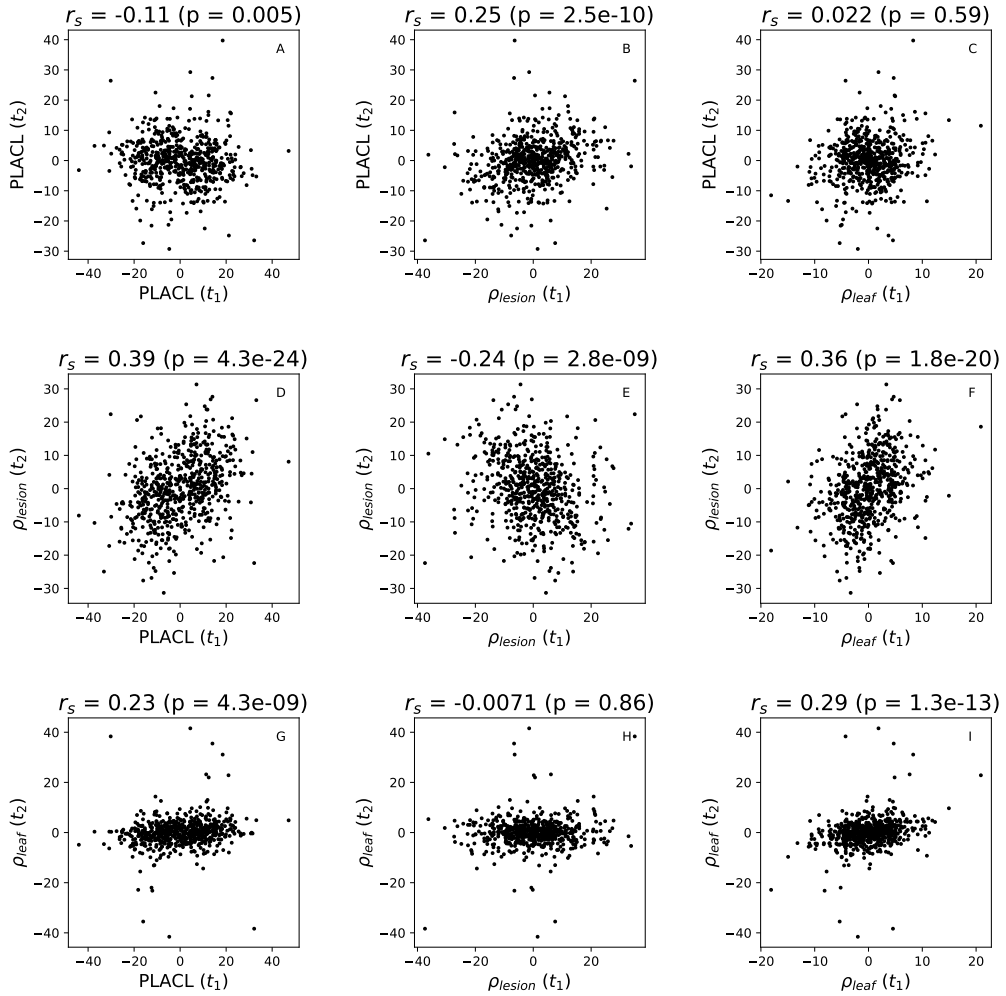

Figure E4.2: Correlation of measures of resistance between t_1 and t_2 within cultivars. Data from each cultivar is represented by two data points. For each point, the x-value represents the difference between the mean over an individual plot and the grand mean over two plots at t_1 and the y-value is the same difference taken at t_2. Each data point represents an average over about 16 leaves of one cultivar belonging an individual plot. The degree of correlation is quantified using Spearman's correlation coefficient, r_s.

bioRxiv preprint doi: https://doi.org/10.1101/129353; this version posted April 29, 2017. The copyright holder for this preprint (which was not certified by peer review) is the author/funder, who has granted bioRxiv a license to display the preprint in perpetuity. It is made available under aCC-BY 4.0 International license.

Literature Cited

Benjamini, Y., and Y. Hochberg. 1995. Controlling the False Discovery Rate: A Practical and Powerful Approach to Multiple Testing. Journal of the Royal Statistical Society. Series B (Methodological) **57**:289–300.

Brading, P. A., E. C. Verstappen, G. H. Kema, and J. K. Brown. 2002. A gene-for-gene relationship between wheat and Mycosphaerella graminicola, the Septoria tritici blotch pathogen. Phytopathology **92**:439–445.

Brokenshire, T. 1976. The reaction of wheat genotypes to Septoria tritici. Annals of Applied Biology **82**:415–423.

Brown, J., G. Kema, H.-R. Forrer, E. Verstappen, L. Arraiano, P. Brading, E. Foster, P. Fried, and E. Jenny. 2001. Resistance of wheat cultivars and breeding lines to septoria tritici blotch caused by isolates of Mycosphaerella graminicola in field trials. Plant Pathology **50**:325–338.

Brunner, P., F. Stefanato, and B. McDonald. 2008. Evolution of the CYP51 gene in Mycosphaerella graminicola : evidence for intragenic recombination and selective replacement. Mol. Plant Pathol. **9**:305–316.

Chartrain, L., P. Brading, J. Makepeace, and J. Brown. 2004. Sources of resistance to septoria tritici blotch and implications for wheat breeding. Plant Pathology **53**:454–460.

Cools, H. J., and B. Fraaije. 2013. Update on mechanisms of azole resistance in Mycosphaerella graminicola and implications for future control. Pest Manag. Sci. **69**:150–5.

de Mendiburu, F., 2016. agricolae: Statistical Procedures for Agricultural Research. URL `https://CRAN.R-project.org/package=agricolae`.

Dean, R., J. A. L. Van Kan, Z. A. Pretorius, K. I. M. E. Hammond-kosack, A. D. I. Pietro, P. D. Spanu, J. J. Rudd, M. Dickman, R. Kahmann, J. Ellis, and G. D. Foster. 2012. The Top 10 fungal pathogens in molecular plant pathology. Mol. Plant Pathol. **13**:414–430.

Deery, D., J. Jimenez-Berni, H. Jones, X. Sirault, and R. Furbank. 2014. Proximal remote sensing buggies and potential applications for field-based phenotyping. Agronomy **4**:349–379.

Drăguţ, L., and T. Blaschke. 2006. Automated classification of landform elements using object-based image analysis. Geomorphology **81**:330–344.

Duncan, K. E., and R. J. Howard. 2000. Cytological analysis of wheat infection by the leaf blotch pathogen Mycosphaerella graminicola. Mycological research **104**:1074–1082.

bioRxiv preprint doi: https://doi.org/10.1101/129353; this version posted April 29, 2017. The copyright holder for this preprint (which was not certified by peer review) is the author/funder, who has granted bioRxiv a license to display the preprint in perpetuity. It is made available under aCC-BY 4.0 International license.

Estep, L., S. Torriani, M. Zala, N. Anderson, M. Flowers, B. McDonald, C. Mundt, and P. Brunner. 2015. Emergence and early evolution of fungicide resistance in North American populations of Zymoseptoria tritici. Plant Pathology **64**:961–971.

Eyal, Z. 1992. The response of field-inoculated wheat cultivars to mixtures of Septoria tritici isolates. Euphytica **61**:25–35.

Fones, H., and S. Gurr. 2015. The impact of Septoria tritici Blotch disease on wheat: an EU perspective. Fungal Genetics and Biology **79**:3–7.

Fraaije, B., H. J. Cools, J. Fountaine, D. J. Lovell, J. Motteram, J. S. West, and J. a. Lucas. 2005. Role of Ascospores in Further Spread of QoI-Resistant Cytochrome b Alleles (G143A) in Field Populations of Mycosphaerella graminicola. Phytopathology **95**:933–941.

Friesen, T. L., J. D. Faris, P. S. Solomon, and R. P. Oliver. 2008. Host-specific toxins: effectors of necrotrophic pathogenicity. Cellular microbiology **10**:1421–1428.

Griffin, M. J., and N. Fisher. 1985. Laboratory studies on benzimidazole resistance in Septoria tritici. EPPO Bull. **15**:505–511.

Jorgensen, L. N., M. S. Hovmoller, J. Hansen, P. Lassen, B. Clark, R. Bayles, B. Rodemann, K. Flath, M. Jahn, T. Goral, J. Jerzy Czembor, P. Cheyron, C. Maumene, C. De Pope, R. Ban, G. C. Nielsen, and G. Berg. 2014. IPM Strategies and Their Dilemmas Including an Introduction to www.eurowheat.org. J. Integr. Agric. **13**:265–281.

Kema, G. H., D. Yu, F. H. Rijkenberg, M. W. Shaw, and R. P. Baayen. 1996. Histology of the pathogenesis of Mycosphaerella graminicola in wheat. Phytopathology **86**:777–786.

Kirchgessner, N., F. Liebisch, K. Yu, J. Pfeifer, M. Friedli, A. Hund, and A. Walter. 2017. The ETH field phenotyping platform FIP: a cable-suspended multi-sensor system. Functional Plant Biology **44**:154–168.

Kollers, S., B. Rodemann, J. Ling, V. Korzun, E. Ebmeyer, O. Argillier, M. Hinze, J. Plieske, D. Kulosa, M. W. Ganal, and M. S. Rder. 2013*a*. Whole Genome Association Mapping of Fusarium Head Blight Resistance in European Winter Wheat (Triticum aestivum L.). PLOS ONE **8**:1–10.

Kollers, S., B. Rodemann, J. Ling, V. Korzun, E. Ebmeyer, O. Argillier, M. Hinze, J. Plieske, D. Kulosa, M. W. Ganal, et al. 2013*b*. Genetic architecture of resistance to Septoria tritici blotch (Mycosphaerella graminicola) in European winter wheat. Molecular breeding **32**:411–423.

Kou, Y., and S. Wang. 2010. Broad-spectrum and durability: understanding of quantitative disease resistance. Curr. Opin. Plant Biol. **13**:181–5.

bioRxiv preprint doi: https://doi.org/10.1101/129353; this version posted April 29, 2017. The copyright holder for this preprint (which was not certified by peer review) is the author/funder, who has granted bioRxiv a license to display the preprint in perpetuity. It is made available under aCC-BY 4.0 International license.

Krattinger, S. G., E. S. Lagudah, W. Spielmeyer, R. P. Singh, J. Huerta-Espino, H. McFadden, E. Bossolini, L. L. Selter, and B. Keller. 2009. A putative ABC transporter confers durable resistance to multiple fungal pathogens in wheat. Science **323**:1360–1363.

Linde, C., J. Zhan, and B. McDonald. 2002. Population structure of Mycosphaerella graminicola: from lesions to continents. Phytopathology **92**:946–955.

Mahlein, A.-K. 2016. Plant disease detection by imaging sensors–parallels and specific demands for precision agriculture and plant phenotyping. Plant Disease **100**:241–251.

Marcussen, T., S. R. Sandve, L. Heier, M. Spannagl, M. Pfeifer, T. I. Wheat, B. B. H. Wulff, B. Steuernagel, K. F. X. Mayer, M. Pfeifer, K. G. Kugler, S. R. Sandve, and B. Zhan. 2014. A chromosome-based draft sequence of the hexaploid bread wheat (Triticum aestivum) genome Ancient hybridizations among the ancestral genomes of bread wheat Genome interplay in the grain transcriptome of hexaploid bread wheat Structural and functional pa. Science (80-.). **345**:1251781–1251788.

McDonald, B. A., and C. Linde. 2002. Pathogen population genetics, evolutionary potential, and durable resistance. Annu. Rev. Phytopathol. **40**:349–79.

McDonald, B. A., and C. C. Mundt. 2016. How Knowledge of Pathogen Population Biology Informs Management of Septoria Tritici Blotch. Phytopathology **106**:948–955.

Miedaner, T., Y. Zhao, M. Gowda, C. F. H. Longin, V. Korzun, E. Ebmeyer, E. Kazman, and J. C. Reif. 2013. Genetic architecture of resistance to Septoria tritici blotch in European wheat. BMC genomics **14**:858.

Mundt, C. C. 2014. Durable resistance: a key to sustainable management of pathogens and pests. Infection, Genetics and Evolution **27**:446–455.

Mutka, A. M., and R. S. Bart. 2015. Image-based phenotyping of plant disease symptoms. Frontiers in plant science **5**:734.

O'Gorman, L., A. C. Sanderson, and K. Preston. 1985. A system for automated liver tissue image analysis: methods and results. IEEE Transactions on biomedical engineering pages 696–706.

Oliver, R. P., T. L. Friesen, J. D. Faris, and P. S. Solomon. 2012. Stagonospora nodorum: from pathology to genomics and host resistance. Annual review of phytopathology **50**:23–43.

Phukpattaranont, P., and P. Boonyaphiphat, 2007. An automatic cell counting method for a microscopic tissue image from breast cancer. Pages 241–244 *in* 3rd Kuala Lumpur International Conference on Biomedical Engineering 2006. Springer.

Poland, J., P. J. Balint-Kurti, R. J. Wisser, R. C. Pratt, and R. J. Nelson. 2009. Shades of gray: the world of quantitative disease resistance. Trends Plant Sci. **14**:21–9.

bioRxiv preprint doi: https://doi.org/10.1101/129353; this version posted April 29, 2017. The copyright holder for this preprint (which was not certified by peer review) is the author/funder, who has granted bioRxiv a license to display the preprint in perpetuity. It is made available under aCC-BY 4.0 International license.

R Core Team, 2016. R: A Language and Environment for Statistical Computing. R Foundation for Statistical Computing, Vienna, Austria. URL `https://www.R-project.org/`.

Rosielle, A. 1972. Sources of resistance in wheat to speckled leaf blotch caused by Septoria tritici. Euphytica **21**:152–161.

Sánchez-Vallet, A., M. C. McDonald, P. S. Solomon, and B. A. McDonald. 2015. Is Zymoseptoria tritici a hemibiotroph? Fungal Genetics and Biology **79**:29–32.

Schindelin, J., C. T. Rueden, M. C. Hiner, and K. W. Eliceiri. 2015. The ImageJ Ecosystem : An Open Platform for Biomedical Image Analysis. Mol. Reprod. Dev. **529**:518–529.

Shaner, G., R. Finney, and F. Patterson. 1975. Expression and effectiveness of resistance in wheat to septoria leaf blotch. Phytopathology **65**:761–766.

Shaner, G., and R. E. Finney. 1982. Resistance in Soft Red Winter Wheat to Mycosphaerella graminicola. Phytopathology **72**:154–158.

Shaw, M. 1990. Effects of temperature, leaf wetness and cultivar on the latent period of Mycosphaerella graminicola on winter wheat. Plant Pathology **39**:255–268.

Simko, I., J. A. Jimenez-Berni, and X. R. Sirault. 2017. Phenomic approaches and tools for phytopathologists. Phytopathology **107**:6–17.

Sokal, R. R., and F. J. Rohlf. 2012. Biometry. W. H. Freeman.

St. Clair, D. A. 2010. Quantitative disease resistance and quantitative resistance loci in breeding. Annual review of phytopathology **48**:247–268.

Stewart, E. L., C. H. Hagerty, A. Mikaberidze, C. C. Mundt, Z. Zhong, and B. A. McDonald. 2016. An improved method for measuring quantitative resistance to the wheat pathogen Zymoseptoria tritici using high-throughput automated image analysis. Phytopathology **106**:782–788.

Stewart, E. L., and B. A. McDonald. 2014. Measuring quantitative virulence in the wheat pathogen Zymoseptoria tritici using high-throughput automated image analysis. Phytopathology **104**:985–992.

Torriani, S. F., P. C. Brunner, B. A. McDonald, and H. Sierotzki. 2009. QoI resistance emerged independently at least 4 times in European populations of Mycosphaerella graminicola. Pest management science **65**:155–162.

Torriani, S. F., J. P. Melichar, C. Mills, N. Pain, H. Sierotzki, and M. Courbot. 2015. Zymoseptoria tritici: a major threat to wheat production, integrated approaches to control. Fungal Genetics and Biology **79**:8–12.

bioRxiv preprint doi: https://doi.org/10.1101/129353; this version posted April 29, 2017. The copyright holder for this preprint (which was not certified by peer review) is the author/funder, who has granted bioRxiv a license to display the preprint in perpetuity. It is made available under aCC-BY 4.0 International license.

Walter, A., F. Liebisch, and A. Hund. 2015. Plant phenotyping: from bean weighing to image analysis. Plant methods **11**:14.

Zadoks, J. C., T. T. Chang, and C. F. Konzak. 1974. A decimal code for the growth stages of cereals. Weed research **14**:415–421.

Zhan, J., C. Mundt, and B. McDonald. 1998. Measuring immigration and sexual reproduction in field populations of Mycosphaerella graminicola. Phytopathology **88**:1330–1337.

Zhan, J., C. Mundt, and B. McDonald. 2000. Estimation of rates of recombination and migration in populations of plant pathogensa reply. Phytopathology **90**:324–326.

Zhan, J., C. C. Mundt, M. E. Hoffer, and B. A. McDonald. 2002. Local adaptation and effect of host genotype on the rate of pathogen evolution : an experimental test in a plant pathosystem. J. Evol. Biol. **15**:634–647.

Zhan, J., R. Pettway, and B. McDonald. 2003. The global genetic structure of the wheat pathogen Mycosphaerella graminicola is characterized by high nuclear diversity, low mitochondrial diversity, regular recombination, and gene flow. Fungal Genetics and Biology **38**:286–297.

Zhan, J., F. Stefanato, and B. McDonald. 2006. Selection for increased cyproconazole tolerance in Mycosphaerella graminicola through local adaptation and in response to host. Mol. Plant Pathol. **7**:259–268.

Zhong, Z., T. C. Marcel, F. E. Hartmann, X. Ma, C. Plissonneau, M. Zala, A. Ducasse, J. Confais, J. Compain, N. Lapalu, et al. 2017. A small secreted protein in Zymoseptoria tritici is responsible for avirulence on wheat cultivars carrying the Stb6 resistance gene. New Phytologist in press .